Tuğba SAĞIR

PHOTODYNAMIC INACTIVATION OF DIFFERENT CANCER CELL LINES BY PROTOPORPHYRIN IX AND ITS DOPAMINE CONJUGATE

by

Tuğba SAĞIR

M.S. Thesis In Biology

December-2010

December 2010

PHOTODYNAMIC INACTIVATION OF DIFFERENT CANCER CELL LINES BY PROTOPORPHYRIN IX AND ITS DOPAMINE CONJUGATE

by

Tuğba SAĞIR

A thesis submitted to

the Graduate Institute of Sciences and Engineering

of

Fatih University

in partial fulfillment of the requirements for the degree of

Master of Science

in

Biology

December 2010
Istanbul, Turkey

APPROVAL PAGE

I certify that this thesis satisfies all the requirements as a thesis for the degree of Master of Science.

Assist. Prof. Dr. Sevim IŞIK
Head of Department

This is to certify that I have read this thesis and that in my opinion it is fully adequate, in scope and quality, as a thesis for the degree of Master of Science.

Assist. Prof. Dr. Sevim IŞIK
Supervisor

Examining Committee Members

Assist. Prof. Dr. Sevim IŞIK _____

Assist. Prof. Dr. Lokman ALPSOY _____

Assist. Prof. Dr. Ramazan ÖZTÜRK _____

It is approved that this thesis has been written in compliance with the formatting rules laid down by the Graduate Institute of Sciences and Engineering.

Assoc. Prof. Dr. Nurullah ARSLAN
Director

PHOTODYNAMIC INACTIVATION OF DIFFERENT CANCER CELL LINES BY PROTOPORPHYRIN IX AND ITS DOPAMINE CONJUGATE

Tuğba SAĞIR

M.S. Thesis – Biology
December 2010

Supervisor: Assist. Prof. Dr. Sevim IŞIK

ABSTRACT

Photodynamic therapy (PDT) is a treatment that includes the administration of a photosensitizing drug, often a porphyrin derivative, followed by irradiation with visible light of specific wavelength(s). Photosensitizers produce a type of reactive oxygen species (ROS) that kills neighboring cells when exposed to a specific wavelength of the light. Reactive oxygen species may induce apoptosis, immune response and vascular shutdown or directly kill tumor cells.

We investigated the Protoporphyrin-IX and Dopamine conjugated protoporphyrin on different cancer cell lines. The concentration-dependent viability and cytotoxicity of cells were measured after Protoporphyrin-IX and Dopamine conjugated protoporphyrin treatment. In addition, we showed that Protoporphyrin-IX and Dopamine conjugated protoporphyrin induce apoptosis by causing DNA fragmentation and phosphatidylserine localization on different cancer cell lines prior to photodynamic treatment. We confirmed our results by checking Caspase-3 activity with Reverse Transcriptase-Polymerase Chain Reaction (RT-PCR).

Keywords: Photodynamic therapy, protoporphyrin IX, apoptosis, cytotoxicity.

FARKLI KANSER HÜCRE SOYLARININ PROTOPORFİRİN IX VE DOPAMİNE KONJUGESİ İLE FOTODİNAMİK İNAKTİVASYONU

Tuğba SAĞIR

Yüksek Lisans Tezi – Biyoloji
Aralık 2010

Tez Danışmanı: Yrd. Doç. Dr. Sevim IŞIK

ÖZ

Fotodinamik tedavi (FDT), genellikle porfirin gibi ışığa duyarlı bir ilâcın intravenöz olarak özel bir dalga boyunda/boylarındaki görünür ışıkla aktive edilerek verilmesiyle gerçekleşen bir tedavi şeklidir. Işığa duyarlı maddeler, belirli bir dalga boyundaki ışığa maruz bırakıldığında, yakınındaki hücreleri öldüren bir reaktif oksijen türü (ROT) oluşturur. Reaktif oksijen türleri apoptoz, immün tepki ve vasküler yıkımı tetikleyebilir veya tümör hücrelerini doğrudan öldürebilir.

Bu çalışmada, Protoporfirin-IX ve Dopamin bağlı protoporfirin farklı kanser hücreleri üzerinde incelendi. Hücrelerin derişime bağlı canlılık ve sitotoksisitesi Protoporfirin-IX ve Dopamin bağlı protoporfirin uygulamasından sonra ölçüldü. Buna ek olarak, Protoporfirin-IX ve Dopamin bağlı protoporfirinin FDT ile beraber farklı kanser hücreleri üzerinde DNA kırıkları oluşumu ve fosfotidilserinin hücre düzeyinde belirlenmesi ile apoptozu tetiklediği gösterildi. Sonuçlar Revers Transkriptaz-Polimeraz Zincir Reaksiyonu (RT-PCR) yöntemi ile Kaspaz-3 aktivitesine bakılarak doğrulandı.

Anahtar Kelimeler: Fotodinamik terapi, protoporfirin IX, apoptoz, sitotoksite.

To my parents and my soulmate who I haven't met yet

ACKNOWLEDGEMENT

I would like to express my appreciation to my supervisor Asst. Prof. Dr. Sevim Işık for guiding me on the biological assays and giving me a new insight on what science actually is and how research is done. I also would like to thank to Assist. Prof. Dr. Ramazan ÖZTÜRK for providing me the chemicals synthesized in his lab for my thesis and his helpful discussions. and along with all of my instructors in Fatih University.

I would like to thank my lab-mates Aysel KARAGÖZ, Nebiyyeh KAMACI, Rukiye KARATEPE, Hilal ŞAHİN, Zeynep ÜLKER, Tuba ŞENEL, Saida AAMMİ, Sezin GÜRKAN and also to my colleagues for their support and friendship during and after our master education and I apologize for my friends whose names I may have forgotten to notice here. Special thanks go to Hakan ATAK who has brought more fun to our lab.

My beloved friends Tuba KUNDURACI, Ayşe DEMİR, Nihal KARAKAŞ, Gülsüm ARIKAN and Fatma Kübra CANITEZ, Zeynep AYDIN had a special part in my research. Of course I cannot forget İsmihan ÖZDEMİR, Fatma GÖRAL, Kübra YILMAZ, Merve ÇELİK, Merve AKGÜN, Tuba KARABEY and my little sister Şule TERZİOĞLU for their moral support.

A lot of people helped me and gave me their contributions, especially Gökhan POLAT and Ayhan YALÇIN who have a special role in my life. But if I may say honestly, I could not be able to finish this research without my mother and father.

TABLE OF CONTENTS

ABSTRACT iii
ÖZ iv
ACKNOWLEDGEMENT vi
TABLE OF CONTENTS vii
LIST OF FIGURES x
LIST OF SYMBOLS AND ABBREVIATIONS xii
CHAPTER 1 INTRODUCTION 1
1.1. History 1
1.2 Overview 2
1.3 Photochemistry of PDT 4
1.3.1 Type I and Type II Mechanisms in PDT 5
1.4 Mechanisms of Cell Death in PDT 7
1.4.1 Induction of Apoptosis 8
1.4.1.1 Mitochondria-mediated Apoptosis 8
1.4.1.2 Death receptor-mediated Apoptosis 11
1.5 Apoptosis Detection Methods 11
1.5.1 Morphological Changes 11
1.5.1.1 Light Microscopy (LM) 11
1.5.1.2 Electron Microscopy (EM) 11
1.5.2 Cytoplasmic Changes 12
1.5.3 DNA Fragmentation 12
1.5.3.1 DNA Laddering 12
1.5.3.2 DNA Content by FC 12
1.5.3.3 DNA Strand Break Labeling 12
1.5.4 Plasma Membrane Alterations 13
1.5.4.1 Membrane Permeability 13
1.5.4.2 Membrane Changes 13

1.5.5 Annexin V 14
1.6 Vascular Effect 14
1.7 Immune Responses 16
1.8 Clinical Applications 17
1.9 PHOTOSENSITIZERS 20
1.9.1 General Properties of Photosensitizers 20
1.9.2 The Fluorescence of Photosensitizers 20
1.9.3 Classification of Photosensitizers 21
1.9.3.1 Porphyrins 22
1.9.3.1.1 Properties of Porphyrins 22
1.9.3.1.2 Protoporphyrin-IX 24
CHAPTER 2 MATERIALS AND METHODS 27
2.1 General 27
2.2 Cell Culture 27
2.2.1 . Thawing Hela, U87, and SH-SY5Y Cells 27
2.2.2 Seeding and Subculture of NB, HeLa and U87 Cells 28
2.2.3 Cell Treatment with (PpIX) and (DPpIX) 28
2.3 Cytotoxicity Assay 31
2.4 Cell Viability Assay 32
2.5 Immunoflourescent Staining 32
2.5.1 Phosphatidylserine Localization 32
2.5.2 DNA Fragmentation 32
2.6 REVERSE TRANSCRIPTION PCR 33
2.6.1 cDNA Synthesis 33
2.6.2 RT-PCR 33
2.6.3 Gel Electrophoresis 34
CHAPTER 3 RESULTS 35
3.1 Cytotoxicity Assay 35
3.2 Proliferation Assay 38
3.3 DNA Fragmentation 39
3.4 Phosphotidylserine Localization 44
3.5 Caspase Activity 52
CHAPTER 4 DISCUSSION 54

CHAPTER 5 CONCLUSION 58
REFERENCES 59

LIST OF FIGURES

Figure 1.1 A simplified representation of events in photodynamic action. 2
Figure 1.2 A proposed model showing the mitochondria as both source and target of ROS and the role in apoptosis induction 3
Figure 1.3 Energy level diagram for the photoexcitation of a molecule 4
Figure 1.4 Jablonski Diagram 5
Figure 1.5 Type I and Type II mechanisms 6
Figure 1.6 Photosensitizer excitation in tumor tissue release of active species. 7
Figure 1.7 Illustration of the main apoptotic signaling pathways involving mitochondria 9
Figure 1.8 The two major apoptotic pathways, the death receptor-mediated, or extrinsic pathway, and the mitochondria-mediated-pathway are represented. 10
Figure 1.9 Tunel assay 13
Figure 1.10 A general apoptosis signaling pathway 14
Figure 1.11 Photodynamic therapy using the photosensitizer WST-09 (Tookad) 15
Figure 1.12 Vascular-targeted photodynamic therapy. 16
Figure 1.13 Immune response 17
Figure 1.14 PDT in an optimal clinical setting 19
Figure 1.15 Schematic illustration of fluorescence excitation and emission spectra of dyes. 21
Figure 1.16 The Structure of Porphyrin 22
Figure 1.17 An example of amphiphilic zinc porphyrin 23
Figure 1.18 Structures of some photosensitizers 24
Figure 1.19 Schematic representation of the synthesis of PPD; i: NHS, DCC, DMAP in DMF at RT 26
Figure 2.1 Serial dilutions of the chemicals 29
Figure 2.2 The treated cells under irradiated and unirradiated conditions 30
Figure 2.3 Electronic absorption spectrum of in DMSO 31

Figure 3.1 Irradiation induced cytotoxic effect of PpIX and DPpIX on HeLa cell line 35
Figure 3.2 Irradiation induced cytotoxic effect of PpIX and DPpIX on SH-SY5Y and U87cell lines. 36
Figure 3.3 Results of the proliferation assay of 5 μg/ml of PpIX and DPpIX 38
Figure 3.4 Positive control Camptotechin-treated HeLa cells observed under A) invert light and B) confocal microscopes. 39
Figure 3.5 HeLa cells observed under light and confocal microscopes. The fluorescence images seen in c and d were obtained as a result of TUNNEL assay. 40
Figure 3.6 Apoptosis assay of HeLa cells which are treated 5 μM DPpIX observed under invert light microscope for A and B, and confocal microscope for C and D. A) Images are at 20X (A and B) and 40X (C and D) 41
Figure 3.7 Apoptosis assay of HeLa cells which are treated 15 μM DPpIX observed under invert light microscope for A and B, and confocal microscope for C and D. A) Images are at 20X (A and B) and 40X (C and D). 42
Figure 3.8 % of cell death observed in 5 and 15 μM DPpIX treated HeLa cells 43
Figure 3.9 The fluorescence image of HeLa cells treated with Camptotechin for 30 s exposure. 44
Figure 3.10 DAPI merge. Results of Annexin-V Alexa 568 assay of HeLa cells under fluorescence microscopy A) without irradiation, and B) with irradiation. Exposure time=30 s 44
Figure 3.11 Results of Annexin-V assay of HeLa cells. A-B) 30 s exposure fluorescence microscope images of HeLa cells treated with 5 μM PP-IX in dark and light. C-D) 30 s exposure fluorescence microscope images of HeLa cells treated with 5 μM DPpIX in dark and light 45
Figure 3.12 Results of Annexin-V assay of HeLa cells. A-B) 30 s exposure fluorescence microscope images of HeLa cells treated with 15 μM PP-IX in dark and light. C-D) 30 s exposure fluorescence microscope images of HeLa cells treated with 15 μM DPpIX in dark and light. 46
Figure 3.13 % of cell death in HeLa cells treated with 15 μM PP-IX in dark and light 47
Figure 3.14 The fluorescence images of U-87 cells treated with Camptotechin for 30 s exposure time 48
Figure 3.15 Results of Annexin-V assay of U87 cells. Fluorescence microscope images of control U87 cells. Exposure time = 30 s. 48

Figure 3.16 Results of Annexin-V assay of U-87 cells. A-B) 30 s exposure fluorescence microscope images of HeLa cells treated with 5 μM PP-IX in dark and light. C-D) 30 s exposure fluorescence microscope images of HeLa cells treated with 5 μM DPpIX in dark and light 49
Figure 3.17 Results of Annexin-V assay of U-87 cells. A-B) 30 s exposure fluorescence microscope images of HeLa cells treated with 15 μM PP-IX in dark and light. C-D) 30 s exposure fluorescence microscope images of HeLa cells treated with 15 μM DPpIX in dark and light 50
Figure 3.18 % of cell death in HeLa cells treated with 15 μM PP-IX in dark and light 51
Figure 3.19 Actin and Caspase-3 expressions of U-87 cells 52

LIST OF SYMBOLS AND ABBREVIATIONS

SYMBOL		ABBREVIATION
DMEM	:	Dulbecco's modified Eagle's medium
FBS	:	Fetal Bovine Serum
CO_2	:	Carbon dioxide
RT-PCR	:	Reverse transcriptase polymerase chain reaction
DMSO	:	Dimethylsulfoxide
mRNA	:	Messenger ribonucleic acid
cDNA	:	Complementary deoxyribonucleic acid
PpIX	:	Protoporphyrin IX
DPpIX	:	Protoporphyrin-dopamine conjugate
PpIX*	:	Irradiated PpIX
DPpIX*	:	Irradiated DPpIX
PDT	:	Photodynamic therapy
ROS	:	Reactive oxygen species
PS	:	Photosensitizers
PS*	:	Activated PS
H_2O_2	:	Hydrogen peroxide
TNF	:	Tumor necrosis factor
LM	:	Light microscopy
EM	:	Electron microscopy
TdT	:	Terminal deoxynucleotidyltransferase
APC	:	Antigen presenting cell
LDH	:	Lactate dehydrogenase
TUNEL	:	Terminal deoxynucleotidyl transferase dUTP nick end labeling

CHAPTER 1

INTRODUCTION

PHOTODYNAMIC THERAPY

1.1 History

Photodynamic therapy (PDT) is newly used tecnnique that is used to treat neoplastic and non-neoplastic diseases. *Photosensitizers* are the chemicals that are found in target tissues and activated during PDT. After Raab discovered that certain wavelengths of light were lethal to paramecia exposed to acridine and certain other dyes, the foundations of the concept were laid as early as the beginning of the 20th century. Following Raab, Tappeiner used these dyes topically for the treatment of skin lesions.

The porphyrins are the mostly investigated type of chemical compounds in PDT today. In 1993, Meyer-Betz researched porphyrins for the accumulation of hematoporphyrin (HP) and in rat tumors and PDT effects following systemic administration. Figge and his colleagues used the fluorescence from these compounds in diagnosis and tumor margin delineation in the late 1940s and 1950s [1]

Lipson and Blades said that PDT was not the parent compound and an impurity in HP that was the tumor-localizing agent [2]. Hematoporphyrin derivative (HPD), a mixture of porphyrins produced by the acid treatment of HP was produced after that. The real composition and structure has not been known yet but in general the active portions consist of porphyrin oligomers with ether and/or ester linkages along with monomeric porphyrins [3-4]. In 1970s and 1980s, of Dougherty and colleagues worked on developing of HPD for laboratory and clinical investigations [5-6].

PDT was used to treat tumors in virtually every anatomic site and most are responsive to this therapy to some extent. In 1987, purified form of HPD was used to treat patients for for a variety of neoplasms for the first time and to date several patients are also treated with PDT by Quadra Logic Technologies, Inc. (now QLT Phototherapeutics, Vancouver, Canada) and American Cyanamid Co. (Pearl River, New York) were the first coperations that supported these first randomized trials [7]. They compared the efficacy of PDT with that of other forms of therapy for bladder, esophageal, and lung cancers. In worldwide, important progress has been achieved in obtaining regulatory approval for a variety of indications. 10 countries approved PDT with PF. In the United States, Canada, and Europe there are other requests for treatment of several other indications with other photosensitizers [53].

1.2 Overview

There are three basic componenets that phtodynamic therapy depends on: photosensitizer, cellular oxygen and light. The light of a specific wavelength activates photosensitizer which is a photoreactive drug. After this activation, reactive oxygen species (ROS) generation (singlet oxygen form) is induced. As a result of ROS formation, direct tumor cell death is obtained [8]. Direct tumor destruction via generation of reactive oxygen is not the only reason for tumor destruction. A secondory event; microvascular disruption and local acute inflammation are also induced by PDT [9].

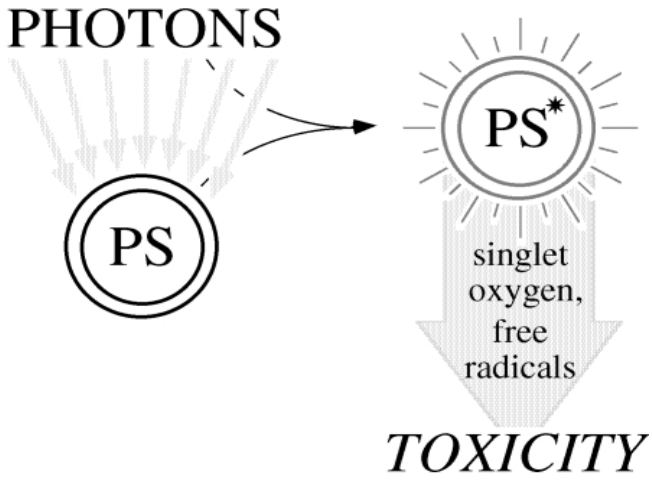

Figure 1.1 A simplified representation of events in photodynamic action [53]

The term ROS is used for short-lived diffusible entities such as hydroxyl (·OH), alkoxyl (RO·) or peroxyl (ROO·) radicals and for some radical species of medium lifetime such as superoxide (O_2·) or nitroxyl radical (NO·). It also includes the non-radicals hydrogen peroxide (H_2O_2), organic hydroperoxides (ROOH) and hypochlorous acid (HOCl). ROS are generated by inflammatory cells, which accumulate in both allergic1 and non-allergic2 inflammations. ROS have destructive actions on both DNA and proteins [10].

ROS may help to cytochrome *c* release because of disruption of the mitochondrial membrane potential.

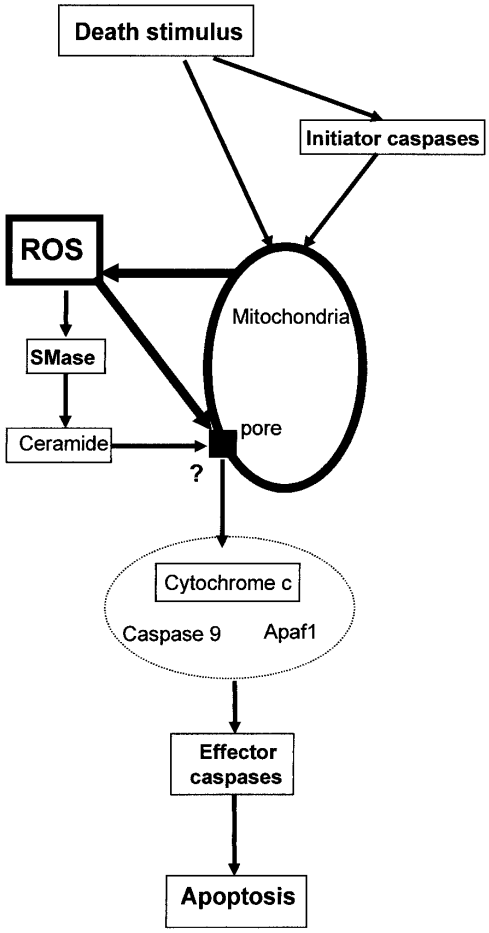

Figure 1.2 A proposed model showing the mitochondria as both source and target of ROS and the role in apoptosis induction [10].

1.3 Photochemistry of PDT

S_0, S_1, and S_2 represent singlet electronic states of the molecule. Excitation of the absorbing molecule from the ground singlet state, S_0, to the first excited singlet state, S_1 is caused by absorption of a of a photon (depicted by hν). S1 directly or from the first triplet excited state, T1, which is generated after intersystem crossing may be reasons for photochemistry. The molecule can relax back to S_0 from either S_1 or T_1 radiatively or nonradiatively. k_{nr}, k_{isc}, k_f, and k_p represent rate constants for nonradiactive decay, intersystem crossing, fluorescence, and phosphorescence, respectively.

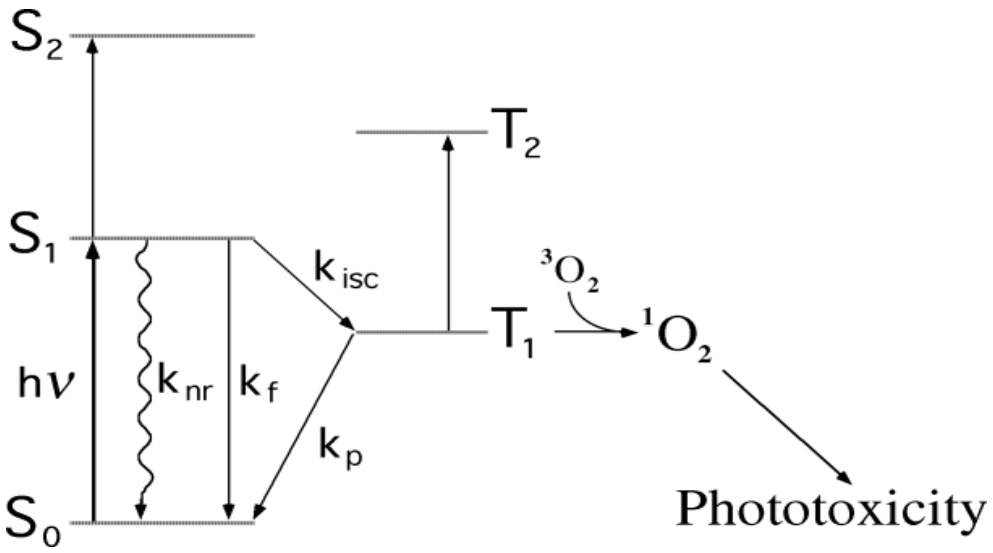

Figure 1.3 Energy level diagram for the photoexcitation of a molecule [53].

After absorption of light energy by a photosensitizer, teh energy of its electrons are increased rendering the photosensitizer excited. By emitting fluorescence, the excited photosensitizer can relax back to its ground state or to a triplet state through a process called intersystem crossing, from which it can relax by emitting phosphorescence. Energy of excited photosensitizer can be transferred to molecular oxygen that is one of the rare compounds which have triplet ground state, and the two molecules relax to respective singlet states in triplet state. Sharman says that in the singlet state molecular oxygen, $^1O_2$, is excited, highly reactive and thereby responsible for the majority of lesions generated during PDT [11]. Excited photosensitizer on

transferring its excess energy returns to its ground state to accept further photons or becomes photochemically degraded (used) in a process referred to as photobleaching. Alternatively, an excited photosensitizer may react directly with biomolecules to form free radicals that further react with molecular oxygen producing superoxide radical anion, hydrogen peroxide or hydroxyl radical. Superoxide radical anion is generated for instance by excitation of porphyrins in the presence of reducing substances [12].

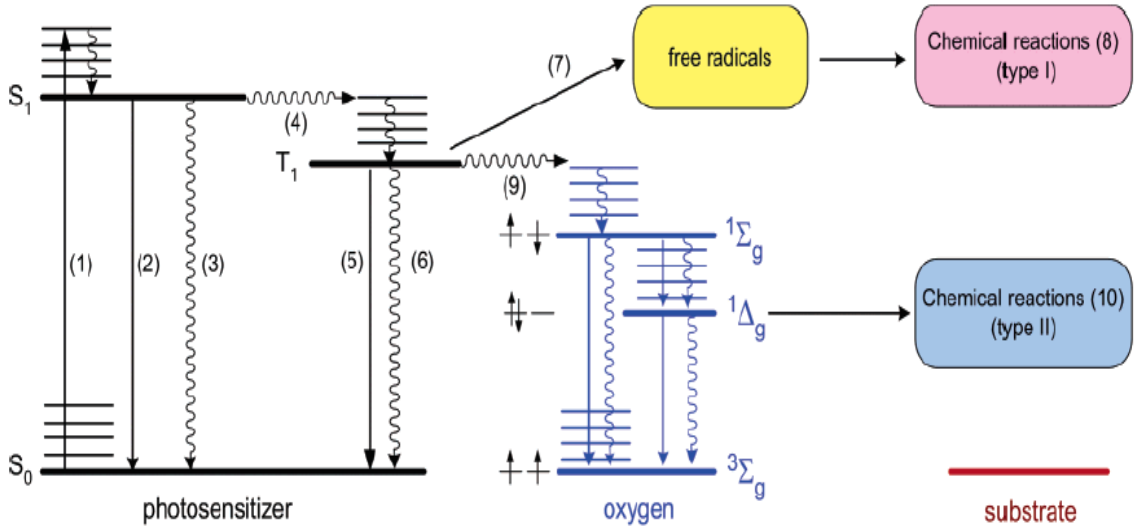

Figure 1.4 Jablonski Diagram [13].

1.3.1 Type I and Type II Mechanisms in PDT

Type I and Type II reactions are two mechanisms by which the triplet state photosensitiser can react with biomolecules.

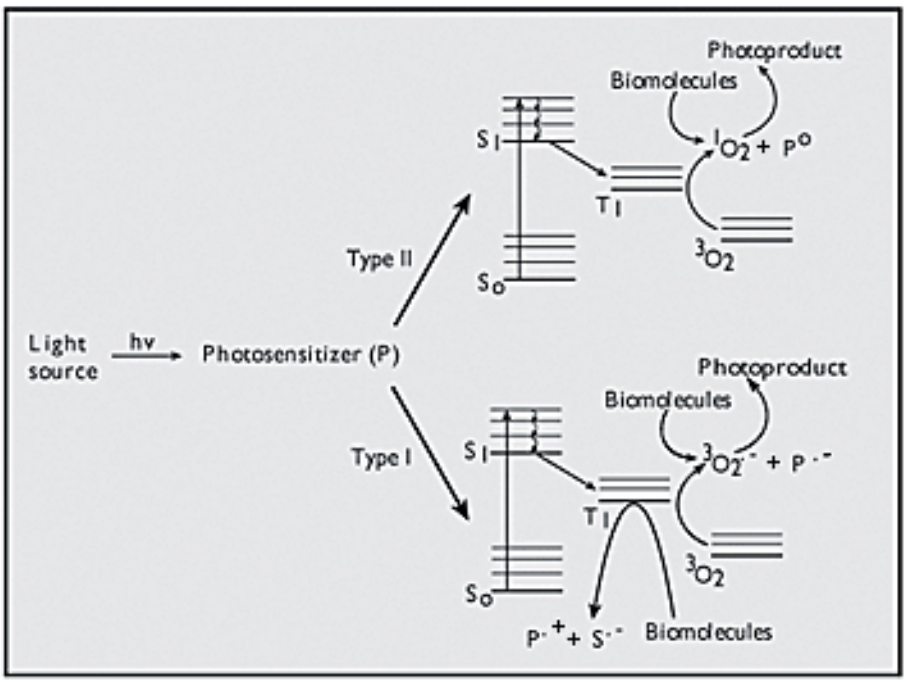

Figure 1.5 Type I and Type II mechanisms [14].

In type I mechanism, electron/hydrogen are transferred directly from the photosensitiser, producing ions, or electron/hydrogen abstraction from a substrate molecule to form free radicals. After rapid reaction of these radicals usually with oxygen, highly reactive oxygen species (e.g. the superoxide and the peroxide anions) are produced. Then, these radicals attack cellular targets.

In type II mechanism, the electronically excited and highly reactive state of oxygen known as singlet oxygen are produced. Direct interaction of the excited triplet state photosensitiser with molecular oxygen (which, unusually, has a triplet ground state) results in the photosensitiser returning to its singlet ground state and the formation of singlet oxygen.

Since very reactive radicalic oxygen species are used, type II mechanism is mostly common mechanism.

1.4 Mechanisms of Cell Death in PDT

There are three interdependent process that cause antitumor effects of PDT: direct tumor cell kill, damage to the vasculature, and activation of a nonspecific immune response [15].

PDT damage to specific subcellular targets and it depenends on the photosensitizer's localization within the cell, which varies among photosensitizers and cell lines. Different types of cell death can be caused by different types of damages such as direct tumor cell photodamage, destruction of tumor vasculature and activation of an immune response. At low light doses, apoptosis can be achieved by damage to to mitochondria [12].

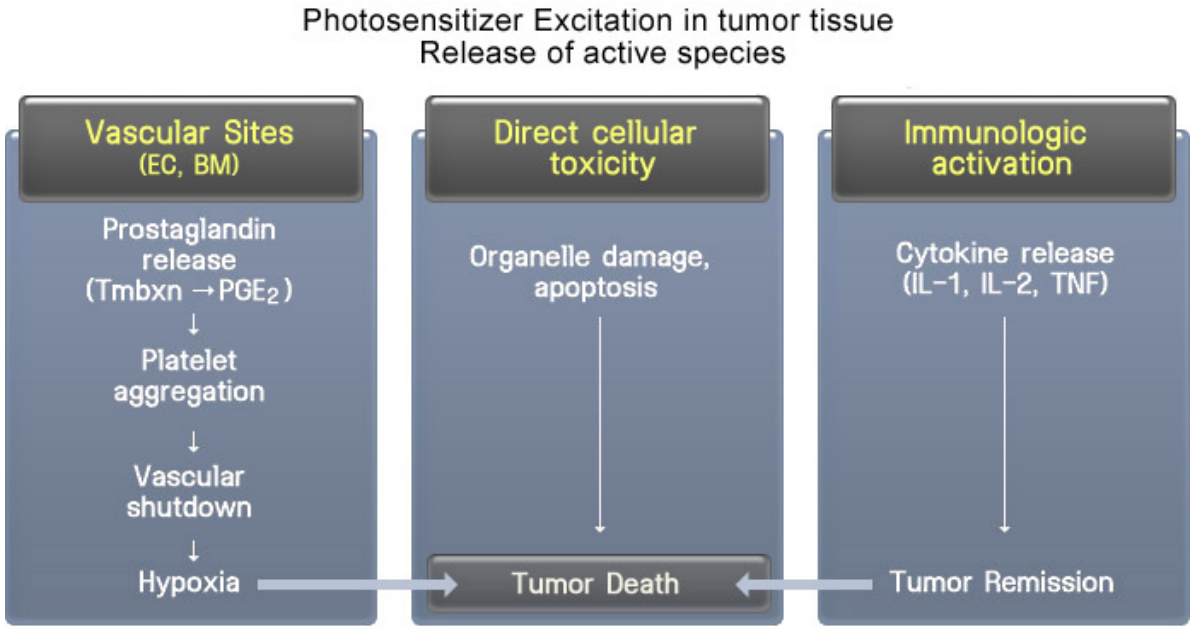

Figure 1.6 Photosensitizer excitation in tumor tissue release of active species [16].

1.4.1 Induction of Apoptosis

Apoptosis is suicidal energy-consuming cell death which is highly controlled and where hydrolytic enzymes such as proteases and nucleases leading to DNA fragmentation and degradation of intracellular structures are activated. Cell shrinkage, chromatin condensation, and production of apoptotic bodies surrounded by neighboring cells and phagocytes are structural features of apoptosis [15].

There are several exogenous and endogenous factors activating apoptosis in biological systems such as oxidative stress, ultraviolet radiation, and genotoxic chemicals. Both intrinsic and extrinsic apoptotic pathways are induced by DNA damage which activates and stabilizes p53 in cytoplasm and nucleus. Although both apoptosis and necrosis are similar in terms of depending on the types, developmental stages, physiological environment of tissues and the nature of death signal, apoptosis is morphologically different from that of necrosis. If the apoptotic pathway fails human diseases like cancer, neurodegenerative and autoimmune disorders may occur.

Potent apopstosis inhibitors of tumor promotion, progression, and the occurrence of cellular inflammatory responses have recently been reported. There are certain photosensitizing drugs used in photodynamic therapy to cause apoptosis for the cancer treatment [17]. Many experimental settings utilizing various photosensitizers and cell types have showed that apoptosis is a fast and a leading cell death form after photodynamic therapy [18]. Apoptosis is triggered *via* two major pathways: mitochondria-mediated or intrinsic pathway and death receptor-mediated or extrinsic pathway by photodynamic therapy [15].

1.4.1.1 Mitochondria-mediated Apoptosis

The use of photosensitizers in mitochondria leads to mitochondrial apoptosis pathway. The disruption of mitochondrial transmembrane potential and cytochrome *c* release to the cytosol are the initial steps of the pathway. This is followed by the

formation of a complex called apoptosome and activation of hydrolytic enzymes — caspases [15].

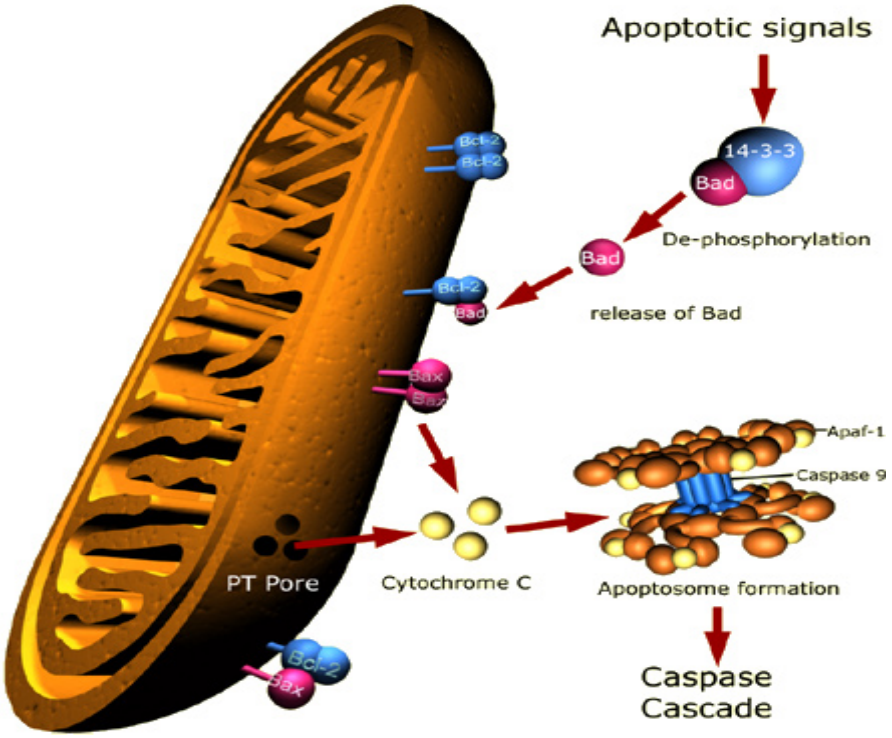

Figure 1.7 Illustration of the main apoptotic signalling pathways involving mitochondria [19].

Role of Caspases in PDT.

The participation of caspases as a cysteine-dependent family of proteases is recognized perhaps the main executional phases of the apoptotic process. Caspases are found within the cell as inactive precursors or zymogens which can be cleaved to form active enzymes following the stimulation of apoptosis [18].

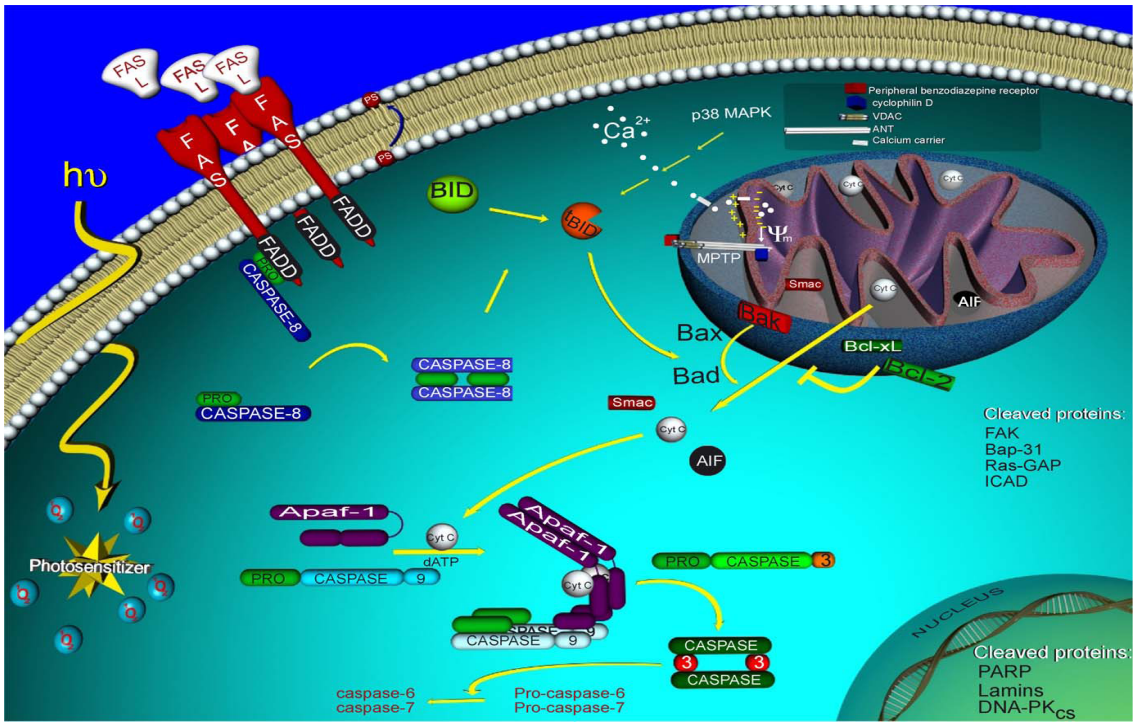

Figure 1.8 Main molecular events causing apoptosis in PDT-treated cells. The death receptor-mediated, or extrinsic pathway, and the mitochondria-mediated-pathway are represented. The results obtained in different tumor models using various sensitizers are shown in the figure [20].

PDT disrupt mithocondrial transmembrane potential and the release of cytochrome c which, when present in the cytoplasm, binds Apaf-1 and procaspase-9 to form a protein complex called apoptosome leading to auto-cleavage and self-activation of caspase-9. Active caspase-9 leads to the cleavage and activation of procaspase-3. After PDT, Caspases 2, -3, -6, -7, and -8 have been shown to be activated in numerous experimental models. Once these hydrolytic enzymes are activated, apoptotic cellular events take place like the cleavage of multiple cellular proteins, DNA fragmentation and even cell death [20-21].

The activation of caspases have been shown to initiate several events on the biochemical level, including DNA laddering (the degradation of DNA into fragments of nearly 200 base pairs), the proteolytic cleavage of cytoskeleton components along with poly (ADP-ribose) polymerase (PARP), and the cell surface exposure of phosphatidylserine (PS) [15].

1.4.1.2 Death Receptor-mediated Apoptosis

The use of photosensitizers targeting the cell membrane is believed to lead to death receptor-mediated apoptosis which is activated when tumor necrosis factor (TNF) binds to cell surface death receptors. Fas receptor is considered to take a major place in PDT triggered apoptosis [22]. The binding of Fas ligand to the clustered death domains through its own death domain leads to the formation of a "death inducing signaling complex" (DISC). DISC is made of Fas, FADD adaptor protein and procaspase-8 which activates itself proteolytically and activates downstream effector caspases [18].

There are other non-extrinsic and non-intrinsic cellular signaling pathways such as calcium homeostasis, ceramide formation and MAPK kinases which may influence PDT-induced apoptosis [15].

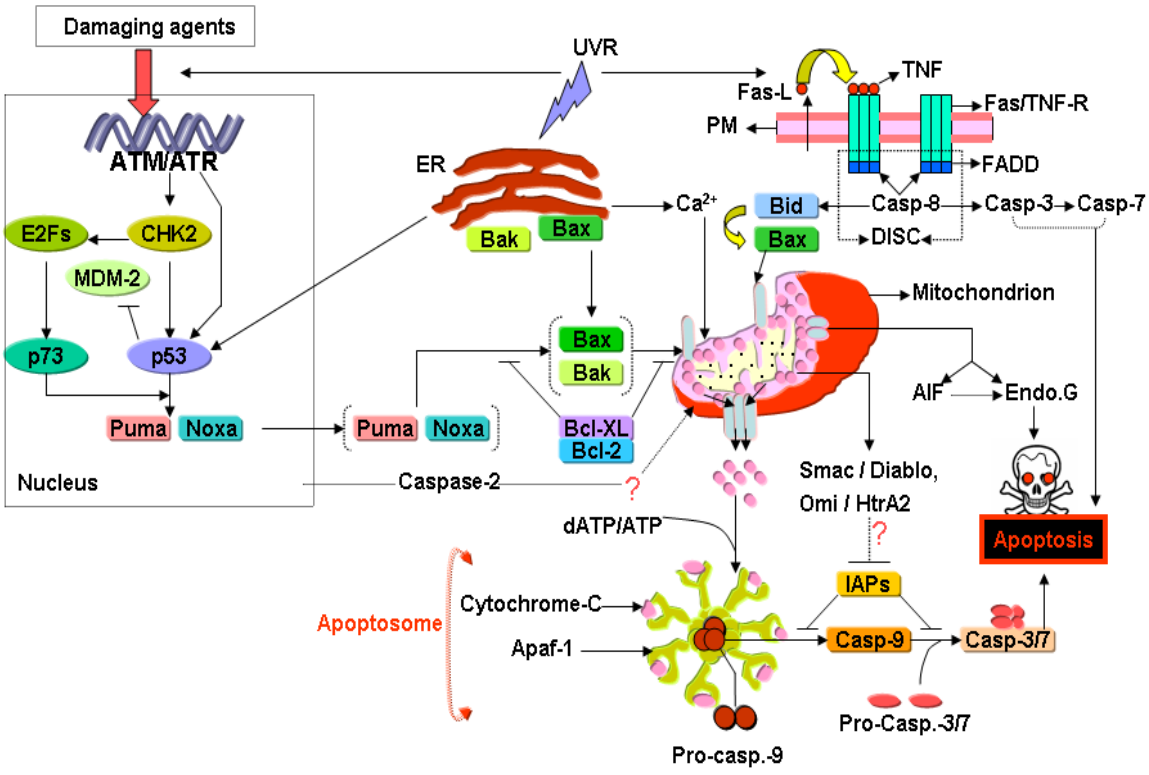

Figure 1.10 A general apoptosis signaling pathway [17].

1.5 Apoptosis detection methods

1.5.1 Morphological Changes

1.5.1.1 Light Microscopy (LM)

Light microscopy is the first and so far the optimum technique for the detection of apoptosis. The main advantages of LM include the visualization of Membrane blebbing, nuclear fragmentation and pyknosis on histological sections stained with eosin and hematoxylin. The low sensitivity of LM however, is a disadvantage due to the detachment of apoptotic cells from the tissues by phagocytosis, which can be completed within 0.5-1 hour once apoptosis has started [23].

1.5.1.2 Electron Microscopy (EM)

Although EM provides a high sensitivity and specificity as compared to LM, it is just a qualitative methodology to detect apoptosis [23].

1.5.2 Cytoplasmic Changes

The vast changes in the biochemistry of the cytoplasm have found good use in terms of the detection of the apoptotic process. Activated enzymes like caspases, different neoepitopes generated by caspase cleavage events, Ca^{2+}-ions, and mitochondrial proteins, which are translocated from the mitochondrion into the cytosolic compartment are some of the cytoplasmic parameters [23].

- Caspase activity
- Calcium flux
- Mitochondrial dysfunction

1.5.3 DNA Fragmentation

1.5.3.1 DNA Laddering

During apoptosis activated endonucleases cleave the chromosomal DNA into fragments of multiples of 180–200 base pairs. These fragments are visualized as a DNA ladder on agarose gels [24].

1.5.3.2 DNA Content by FC

Apoptotic cells show a sub G0/G1 population seen to the left of the G0/G1 peak which can be measured by FC and DNA probes like propidium iodide [23].

1.5.3.3 DNA Strand Break Labeling

The detection of DNA strand breaks resulting from fragmentation of nuclear DNA by the caspase-activated DNase in apoptosis is usually performed by the incorporation of halogenated DNA precursors. Modified nucleotides biotin-, digoxigenin- or fluorescein-labeled dUTP are coupled enzymatically to the 3'-OH ends of DNA strands in the presence of exogenous deoxynucleotidyltransferase (TdT) or DNA polymerase for visualization of apoptotic cells.

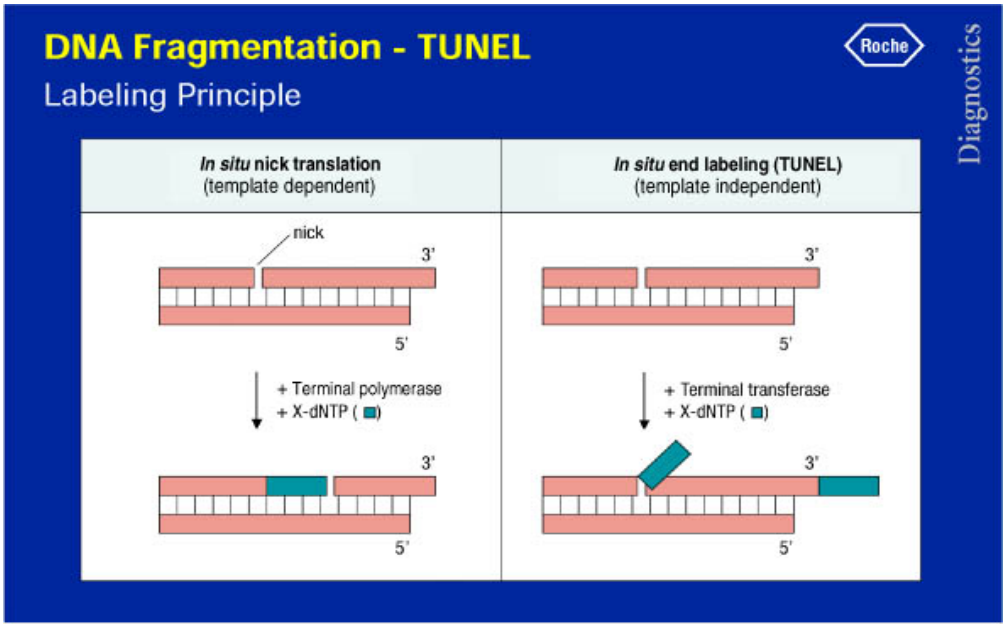

Figure 1.9 Tunel assay [61].

1.5.4 Plasma Membrane Alterations

1.5.4.1 Membrane Permeability

Apoptotic cells show a low uptake of cationic dyes such as trypan blue and propidium iodide (PI). Apoptosis is marked by altered cell morphology while the plasma membrane excludes the uptake

1.5.4.2 Membrane Changes

Apoptotic cells express phosphatidylserine (PS) on their outer leaflet, which is accessible to derivatisation with fluorescamine to derivatize only outer leaflet aminophospholipids analyzed by two-dimensional thin layer chromatography [25].

1.5.5 Annexin V

In 1992, Fadok et al. developed a new apoptosis detection method by demonstrating that apoptotic cells expose PS at their cell surface [25]. Fadok's study urged scientists to establish a novel technique to measure apoptosis using Annexin V. Annexin V is a Ca^{2+}-dependent protein that can conjugate to PS-exposing membranes [26]. Binding of Annexin V to detectable prosthetic groups, like fluorescein and biotin, thus permits the detection of PS exposed cells [27].

1.6 Vascular Effect

The growth of solid tumors is dependent on their capacity to trigger angiogenesis and to acquire blood supply of tumor cells with oxygen and nutrients. So, the development of angiogenesis inhibitors that stop the process of neovascularization in solid tumors is in interest.

It has been known that PDT-induced vascular damage, along with the direct cytotoxicity of PDT, provides another mechanism to treat solid tumors [28]. Preclinical studies show that the mechanisms underlying the vascular effects differ greatly with PDT approaches, photosensitizers, and target tissues [29].

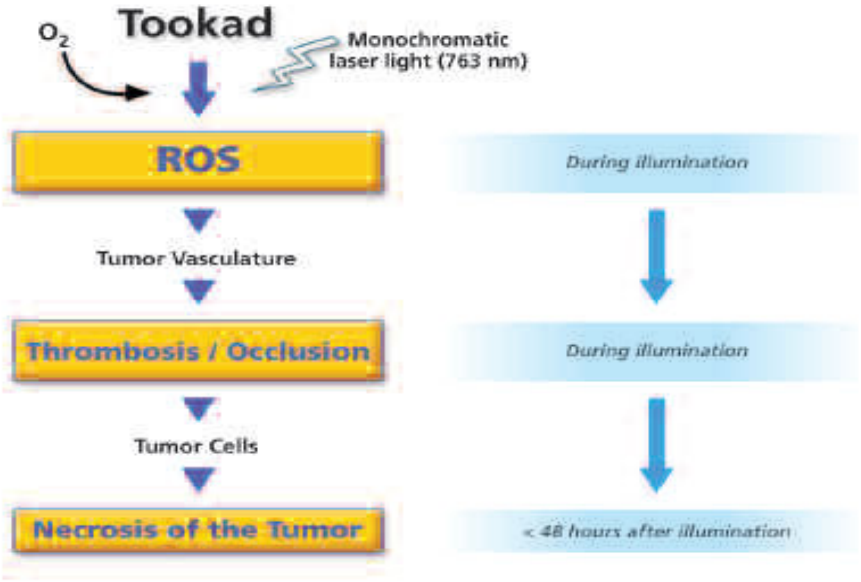

Figure 1.11 Photodynamic therapies using the photosensitizer WST-09 (Tookad) [59].

PDT of tumors achieves a dual selectivity by photosensitizer localization and light delivery by directly targeting the tumor area with light wavelengths specifically absorbed by the photosensitizer. The excited photosensitizer produces highly reactive oxygen species that provoke irreversible neoplastic cell and vessel damages. After the accumulation and irradiation of the sensitizer, the damage to sensitive sites within the microvasculature, i.e. to endothelial cells and the vascular basement membrane, is triggered and leads to the establishment of thrombogenic sites within the vessel lumen. This starts a physiological cascade of responses like platelet aggregation, leukocyte adhesion, vasoactive molecule release, growth in vascular permeability and vessel constriction. This is followed by the tumor destruction by vascular collapse, blood flow stasis and tissue hemorrhages as a result. There are many photosensitizers that can induce serious vasculature damage by a variety of different mechanisms [30].

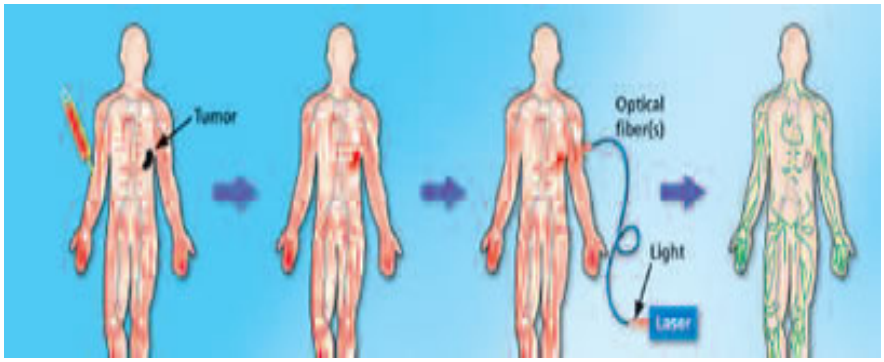

Figure 1.12 Vascular-Targeted Photodynamic therapy [59].

1.7 Immune Responses

Animal studies show that PDT induce immune responses in animal models, their mechanisms and potential impacts by forming pro-inflammatory damages in cellular membranes and the blood vessel walls of treated sites followed by the increase in neutrophils, mast cells and monocytes/macrophages after PDT. More inflammatory mediators to enable massive recruitment of immune cells to tumor site can be released by these cells. Nonspecific immune effector cells and these immune cells have an important effect of tumor destruction [31]. The expression and production of several cytokines, such as IL-1β, IL-2, IL-6, IL-10, TNF-α, and G-CSF can also be triggered by PDT. These cytokines can participate in regulating host immune response including both lymphoid and non-lymphoid cells. According to recent human trials, PDT could improve the uptake and presentation of tumor antigens by tumor-associated antigen presenting cells (APC) and could guarantee the involvement of lymphocytes [32]. Complementactivating agents may further enhance the antitumor effect of PDT [33].

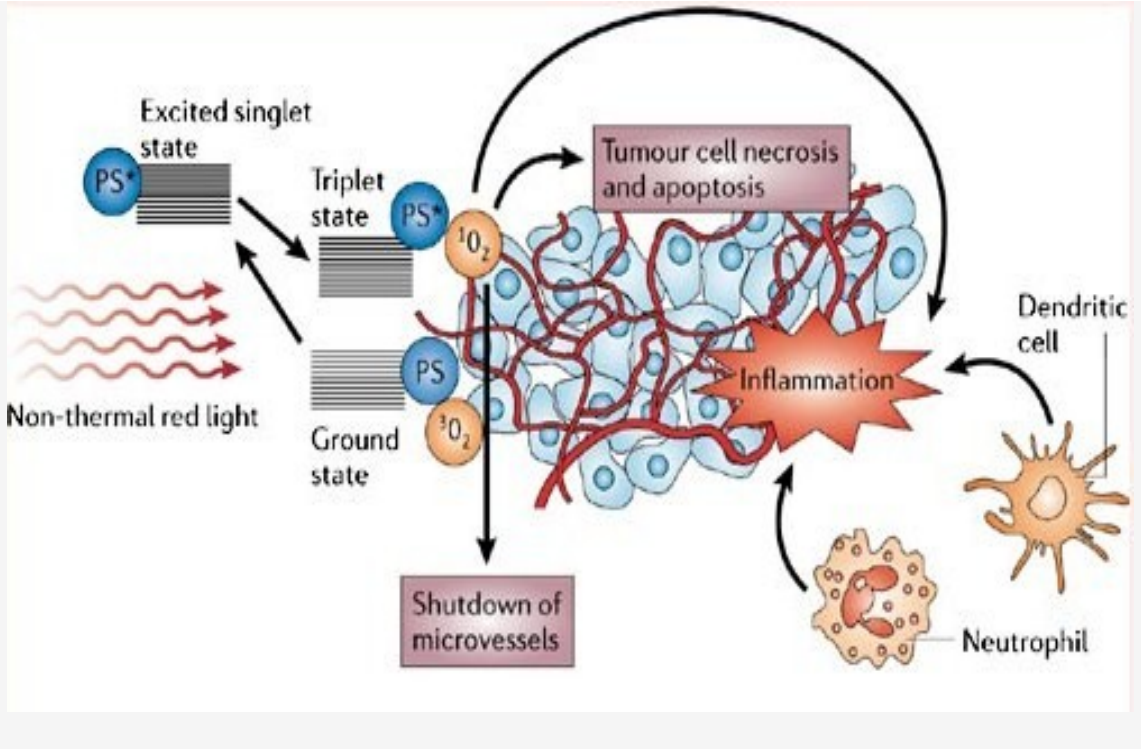

Figure 1.13 Immune response [34].

The mechanism of action of photodynamic therapy is represented in Figure 3.13: The photosensitizer (PS) is excited to the first shortlived excited singlet state by light of a specific wavelength. Next, the excited electron changes its spin and undergoes intersystem crossing to produce a longer-lived triplet state. The energy from the PS is transferred to ground-state triplet oxygen, which produces reactive singlet oxygen ($^1O_2$). $^1O_2$ will very rapidly react with any nearby biomolecules, destruct tumor vasculature and produce an acute inflammatory response that attracts leukocytes such as neutrophils and dendritic cells.

1.8 Clinical Applications

Cancer is a diseases in which abnormal cells divide out of control and they can invade other tissues. These cells can spread to other parts of the body through the blood and lymph systems. Cancer is not just a simple disease but there are more than 100 different types of cancer. Breast cancer, colon and rectal cancer, endometrial cancer, kidney (renal cell) cancer, leukemia, lung cancer, melanoma, non-Hodgkin's lymphoma, pancreatic cancer, prostate cancer, skin cancer (non-melanoma) and thyroid cancer are diagnosed with the highest frequency in developed countries.

In the USA, according to the reports from the nation's leading cancer organizations, cancer death rates have decreased about 2.1 percent per year from 2002 through 2004, nearly twice the annual decrease of 1.1 percent per year from 1993 through 2002. 1,437,180 new cases and 565,650 deaths from cancer are estimated only in the United States in 2008 (National Cancer Institute). Traditional cancer therapies such us radiation therapy, surgery, and chemotherapy are effective but they are not selective in removing malignant cells that spread to normal healthy tissues.

Because of their nonselective cytotoxic properties the conventional chemical and radiation treatments result in serious side effects caused by the loss of normal cell function. They are able to kill the tumor cells but also they are highly detrimental to the patient. That is why devoloping selective treatment protocols that display more effective discrimination of normal and diseased tissue is very important. Some new treatments are: biological therapies for cancer, angiogenesis inhibitor therapy, gene therapy for cancer, bone marrow transplant and peripheral blood stem cell transplant, , laser treatment, photodynamic therapy and targeted cancer therapies.

Photodynamic therapy, PDT, was first suggested 25 years ago as a functional therapeutic approach in oncology. Althuogh it is a promising method to fight cancer, it has only recently begun to be more widely used in clinical practice [35]. Several improvements have occured in the understanding of the chemistry and biology of this treatment method and improved photosensitizing drugs are currently under development. Also, there are some modern light delivery systems.

Currently, it is stated that PDT often has several advantages over surgery and radiotherapy;

- less invasive, has comparable clinical outcome,
- reduced side effects,
- applicability even in areas previously exposed to ionizing radiation,
- relatively short healing times,
- possibility of treatment of various lesions simultaneously,
- possibility to repeat the procedure without risk of developing tumor resistance [36].

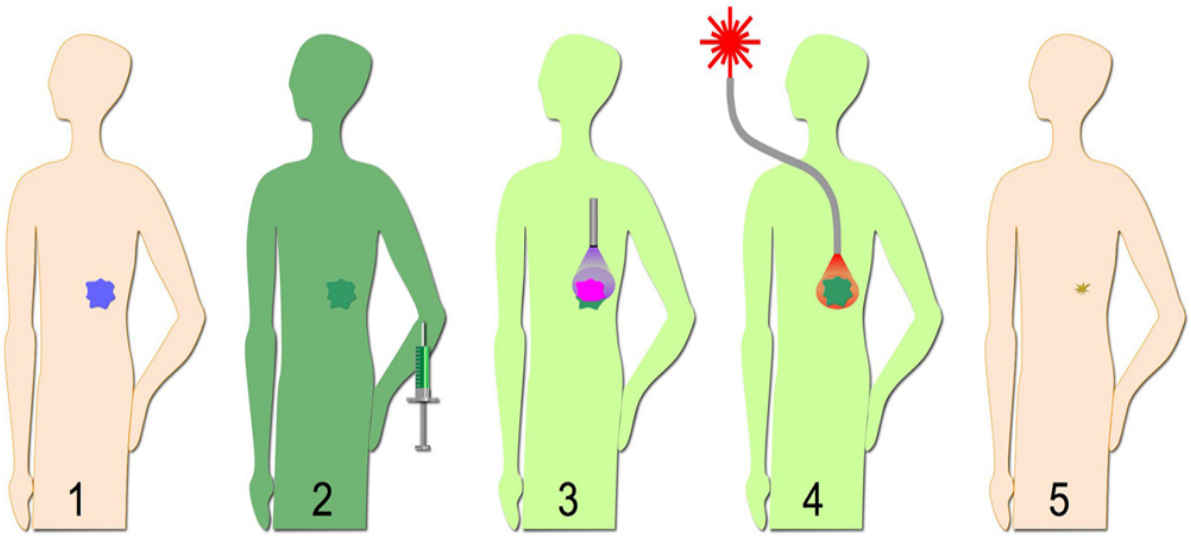

Figure 1.14 PDT in an optimal clinical setting.

(1) A patient with a solid malignant tumor

(2) receives an intravenous injection with a PS

(3) that gets distributed throughout the body and localizes with preference to the tumor. During a waiting period the PS is cleared from most of the body while being retained in the tumor. At this time, fluorescence diagnosis may be used for e.g. PS quantification

(4) After the light exposure

(5) the tumor regresses over time with minimal scarring [60].

1.9 PHOTOSENSITIZERS

1.9.1 General Properties of Photosensitizers

A photosensitizer is a chemical, which upon absorption of light induces a chemical and physical alteration of another chemical.

The photosensitizer is chosen according to the cancer type and it is given to the patient. After a period of time, the tumor is irradiated with appropriate light depending on the photosensitizer and the need to provide the maximum concentration in the malignant tissues. The photosensitizer obtains energy from absorbed light and transfers it to the oxygen molecules that form cytotoxic species to damage the surrounding cells [36].

An ideal photosensitizer should meet at least some of the following criteria:

- a commercially available pure chemical,
- low dark toxicity but strong photocytotoxicity,
- good selectivity towards tumor cells,
- longer wavelength allowing deeper light penetration,
- rapid removal from the body, and
- multiple administration routes (oral, intravenous, intratumoral or inhalational) [29].

1.9.2 The Fluorescence of Photosensitizers

Almost all photosensitizers emit energy from the first excited singlet state as fluorescence. It is known that the energy of light is inversely proportional to the wavelength. The emitted light usually has less energy than the absorbed light therefore the emitted light is usually of higher wavelength. Two spectra, the fluorescence excitation and emission spectra, are usually measured when the fluorescence properties of photosensitizers are evaluated.

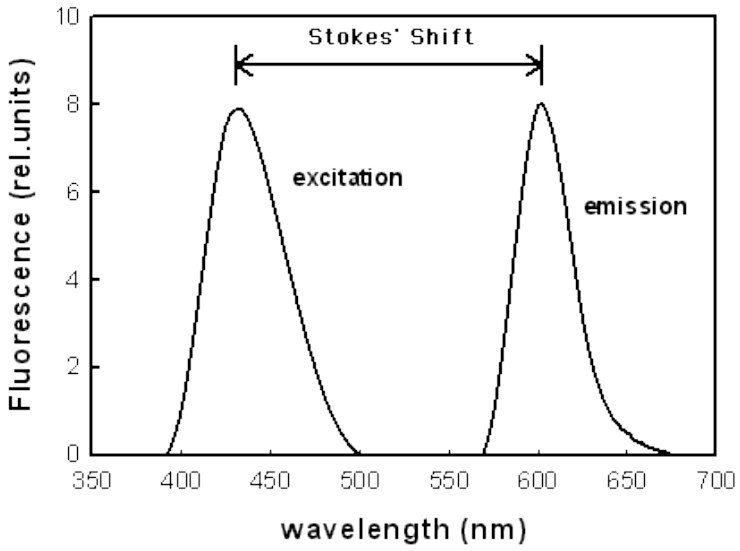

Figure 1.15 Schematic illustration of fluorescence excitation and emission spectra of dyes [54].

When the excitation wavelength is kept constant, and the wavelength for the detection of fluorescence is varied, a fluorescence emission spectrum is obtained. The difference between the excitation and emission peak is the Stoke's shift.

1.9.3 Classification of Photosensitizers

Photosensitizers are usually classified into two groups, porphyrins and nonporphyrins.

Porphyrin-derived photosensitizers are further classified as first, second or third generation photosensitizers. First generation photosensitizers include hematoporphyrin derivative (HpD) and Photofrin. A number of second generation photosensitizers have been developed to alleviate certain problems associated with first generation molecules such as prolonged skin photosensitization and suboptimal tissue penetration [37]. These second generation photosensitizers are chemically pure compared with first generation compounds, absorb light at a longer wavelength and cause significantly less skin photosensitization post-treatment.

In addition, second generation compounds must be at least as efficient in eradicating tumors as Photofrin, the current gold standard for PDT [38]. Second generation photosensitizers bound to carriers such as antibodies and liposomes for selective accumulation within tumor tissue are referred to as third generation photosensitizers and currently represent an active research area in the field [39].

About 30 different photosensitizers which are tetrapyrrole derivatives are used in preclinical studies. Porphyrins, identified over 150 years ago, are the most used photosensitizers because of their minimal toxicity in the dark and a lack of pharmacological interactions with other drugs. These features make PDT a safe procedure in oncological combination treatments [15].

1.9.3.1 Porphyrins

1.9.3.1.1 Properties of Porphyrins

The name of porphyrin is derived from the Greek word for purple.

Porphyrins are a class of tetrapyrroles which include a major component of hemoglobin and myoglobin.

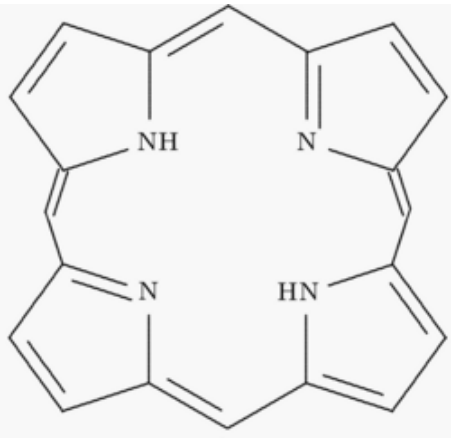

Figure 1.16 Structure of Porphyrin

Porphyrins are vital for the biological activity of all living organisms. Porphyrins have a highly conjugated, heterocyclic macrocycle and may also contain a central metallic atom such as ferrous iron and magnesium [40].

They are extremely important organic compounds and have a vital process. For instance, the vitamin B12 consists of a porphyrin molecule with a cobalt ion in the core.

Porphyrins are amphiphilic organic compounds which have both hydrophilic and hydrophobic parts. Amphiphilicity is having a polar, water-soluble group bound to a non-polar water-insoluble hydrocarbon chain. Amphiphilic photosensitizers are usually more photodynamically active than symmetrically hydrophobic or hydrophilic molecules [41].

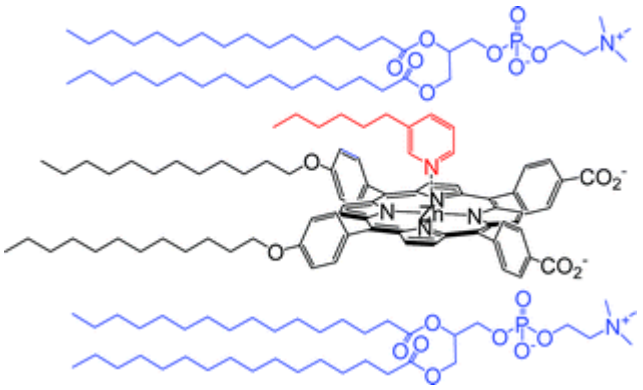

Figure 1.17 An example of amphiphilic zinc porphyrin [42].

The function of the lipophilic side of a photosensitizer is determining the localization and therefore, the site of the cancerous cells. Lipophilic photosensitizers usually accumulate in the membrane and organelles of a cell. The hydrophilic side, as well as agglomerated area of photosensitizers, also penetrate into the cell by pynocitosis and aggregate mainly in lysosomes and endosomes. It was reported by Maria and Julio that the efficiency and selectivity of tumor targeting increases slightly upon increasing the length of the alkyl groups.

Porphyrin IX species such as deuteroporphyrin IX, haematoporphyrin IX, haematoporphyrin derivative, mesoporphyrin IX and protoporphyrin IX are commonly used photosensitizers in photodynamic therapy (PDT), as a new method for cancer treatment [43-44].

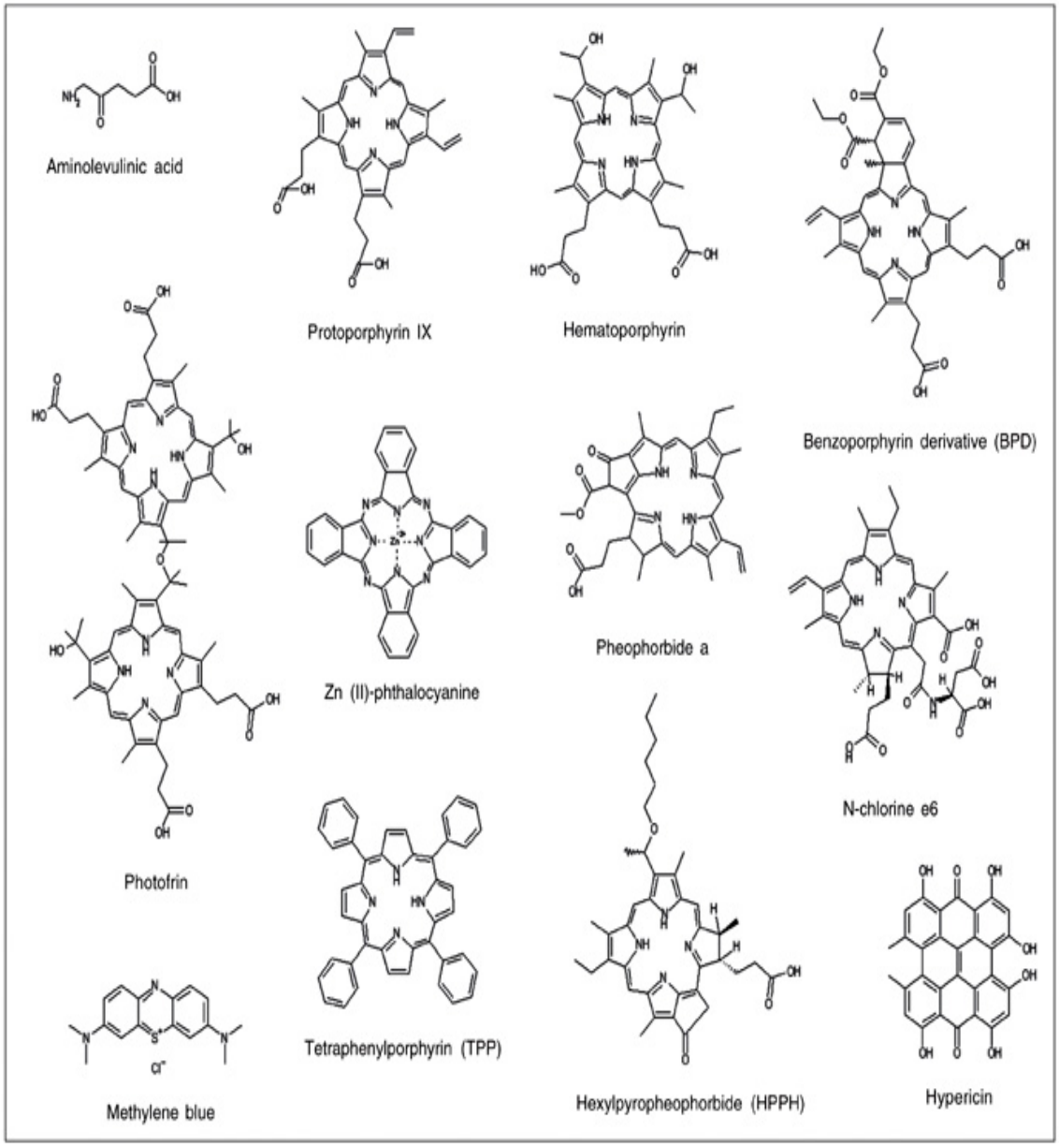

Figure 1.18 Structures of some photosensitizers [45].

1.9.3.1.2 Protoporphyrin-IX

Protoporphyrin-IX (PP-IX, **1**) is known as the `first' porphyrin. Its iron(II) complex, heme, is the prosthetic group for a number of critically important heme proteins such as hemoglobins, myoglobins, cytochromes, catalases and peroxidases. PPIX is also a biosynthetic precursor of chlorophylls and bacteriochlorophylls. X-Ray

studies show that the vinyl-bearing rings of PP-IX are deeply embedded in the protein pockets of heme proteins and that is why the acid groups point to the polar outside of the protein cleft [46].

The most reactive molecule among the porphyrinic photosensitizers towards to conjugate formation is Protoporphyrin (PpIX). It is commonly used in photodynamic therapy (PDT) [47]. In preclinical and clinical studies, PDT applications for cancer treatment, is based on the endogenous accumulation of protoporphyrin IX which is used as a precursor photosensitizer [48].

It was found that patients with malignant tumor have strong basal metabolism and anaerobic respiration, that results in the increased concentration of lactic acid in the body. Local protoporphyrin concentration in tumor is higher than that in the normal tissue because protoporphyrin has higher liposolubility in acidic solution, therefore [49].

By the conjugate formation with biomolecules, the increase of the accumulation of porphyrin photosynthesizers against biological substrates can be achieved [50-51]. For this purpose, ene-diol containing compounds (e.g. dopamine, catechol) are common in nature and they play key roles in many biological reactions and in medical treatment. They also result in altered optical properties of nanoparticles. Dopamine has the ability to replace the original capping ligand, oleylamine, on the Fe_3O_4 NPs surface and act as a robust anchor on the surface of Fe_3O_4 NPs. Moreover, the exceptional thermal stability of the dopamine based anchor on the iron oxide surfaces satisfies the requirement of HT (hyperthermia) [52].

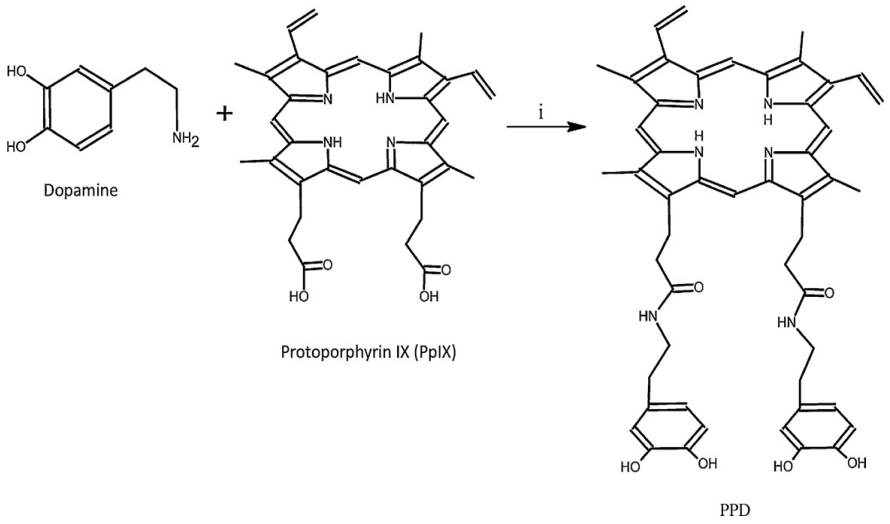

Figure 1.19 Schematic representation of the synthesis of PPD; i: NHS, DCC, DMAP in DMF at RT, 3 h [48].

CHAPTER 2

MATERIALS AND METHODS

2.1 General

The irradiation experiments were performed with 10 Philips TLK 40W/10R lamps (λmax 420 nm) having the light intensity 10mW/cm^2 measured by photometer. Protoporphyrin IX (PpIX) was purchased from Frontier Scientific Europe Carnforth, Lancashire, LA61DE United Kingdom, and protoporphyrin-dopamine conjugate (DPpIX) was prepared according to the given procedure in the literature [48].

2.2 Cell Culture

2.2.1 Thawing Hela, U87, and SH-SY5Y Cells

Before thawing process, 10 ml of pre-warmed DMEM to 37ºC was added into 15 ml falcon tubes. Then cryovial tubes were taken from the nitrogen tank and transferred to 37ºC water bath. As soon as possible, liquid content in the tube was transferred to the tube containing medium and centrifuged at 1500 rpm for 10 min. The supernatant was discarded and the pellet of the cells was resuspended in 10 ml medium and centrifugation was repeated once more in order to get rid of DMSO. All of the cells in the pellet were seeded with DMEM containing 10% FBS and the next day medium was refreshed in order to get rid of dead cells.

2.2.2 Seeding and Subculture of NB, HeLa and U87 Cells

After seeding of cells into culture flasks, cells were attached to the surface of flasks. When cells became 80-90% confluent they were subcultured. Before the subculture, water bath was used to warm DMEM, FBS, PBS and trypsin to 37^{o}C. Medium in the flask was removed by a sterile pipette and then 5 ml of calcium and magnesium free Phosphate Buffered Saline (PBS, Biochrom) to remove residual medium. After removal of PBS, 4 ml of pre-warmed 0.25% Trypsin/EDTA (GIBCO) was added to the flask and kept at room temperature for 1-2 min. Then cells were observed under invert microscope. When cells were detached from the surface of the flask, 1 ml of FBS added to the flask to inactivate the function of trypsin. The cells in the flask with trypsin and FBS was transferred into a new 15 ml falcon tube and centrifuged at 1500 rpm for 10 min at room temperature. After centrifugation, supernatant was discarded by leaving about 0.5 ml of the cell suspension at the bottom. Pellet was finger mixed and volume was up to 10 ml with DMEM medium in order to remove the remaining any tyripsin. Centrifugation step was repeated once more and then cells were counted by hemocytometer. After counting, Hela, NB and U87 cells were seeded at a density of 1500 cells/cm2 with 10% FBS containing DMEM for expansion. Subculture of cells was repeated at about 5-6 days intervals.

2.2.3 Cell Treatment with (PpIX) and (DPpIX)

Cells were seeded at a density of 7,5x10^{3} into 96 well plate. After 24 hrs serial dilutions of the chemicals protoporphyrin IX (PpIX) and protoporphyrin-dopamine conjugate (DPpIX) were prepared at a ratio of 1:1, 1:5, 1:15, 1:30.

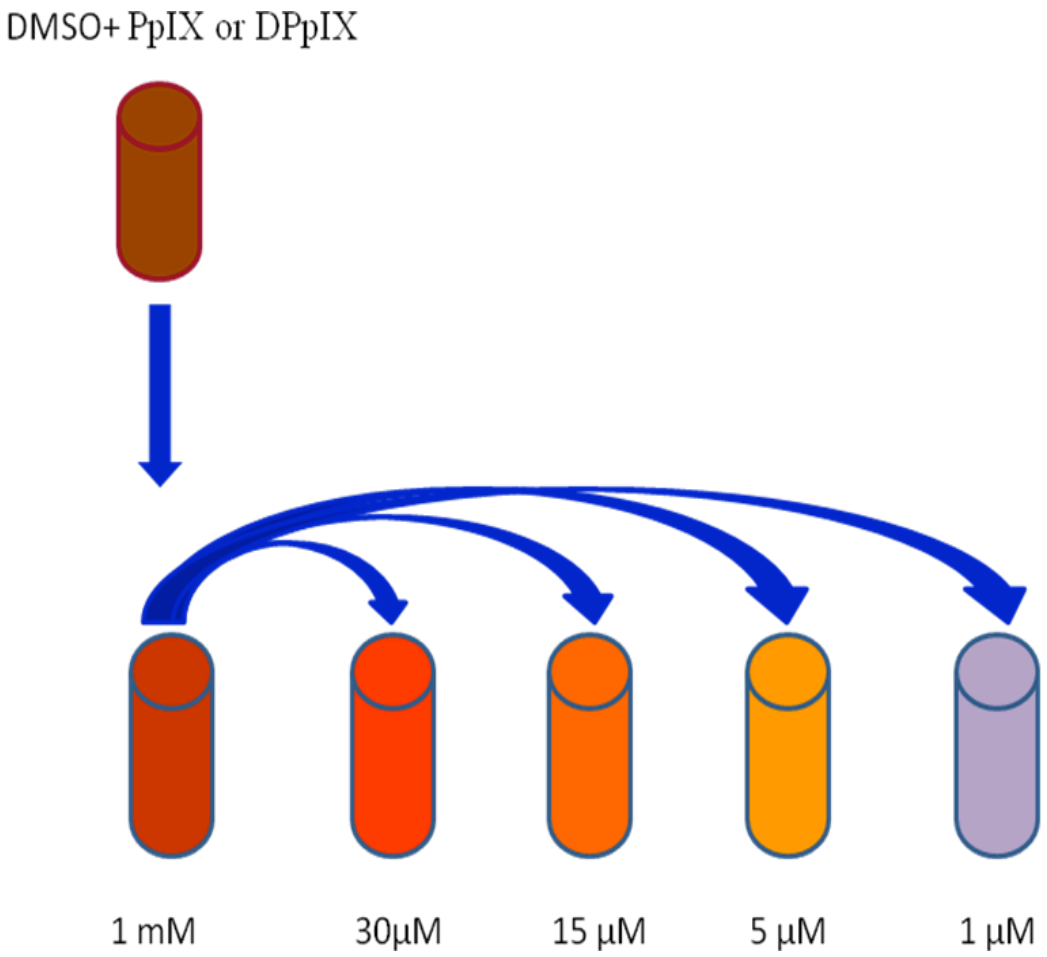

Figure 2.1 Serial dilutions of the chemicals.

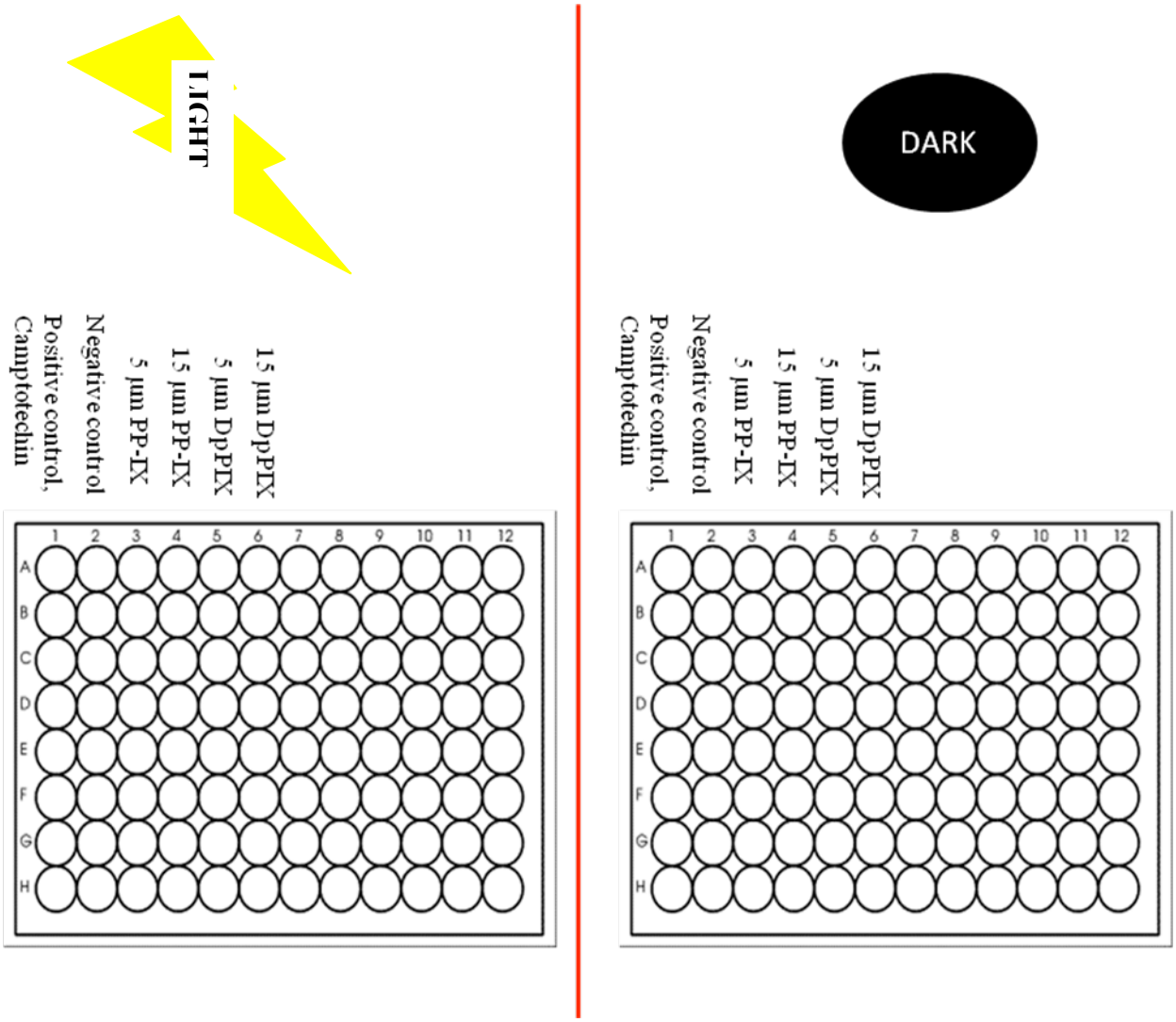

Figure 2.2 The treated cells under irradiated and unirradiated conditions.

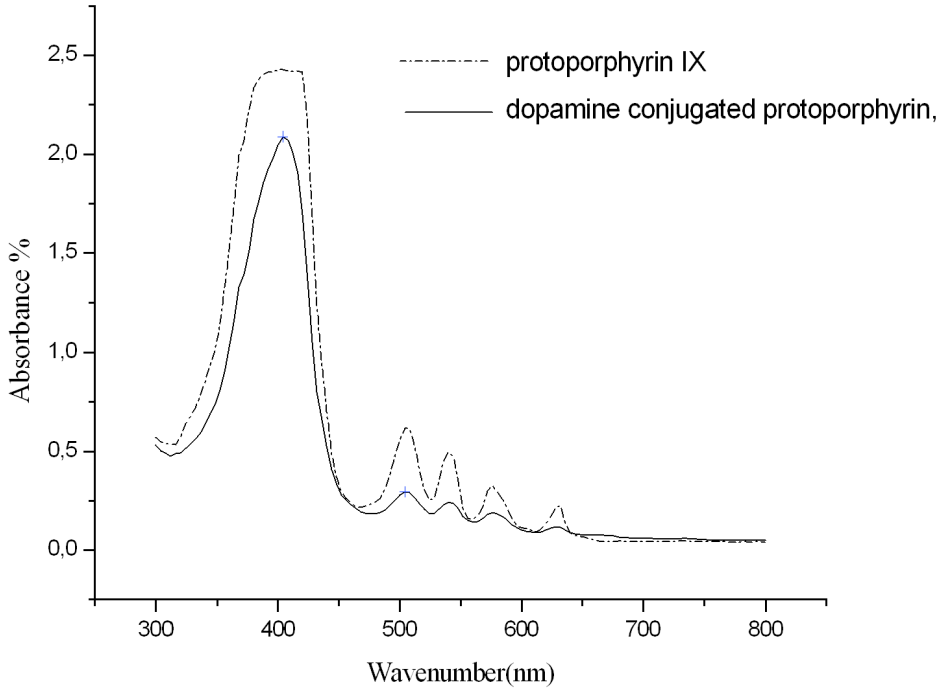

Figure 2.3 Electronic absorption spectrum of in DMSO

2.3 Cytotoxicity Assay

Hela, SH-SY5Y and U87 cell lines were seeded in duplicate 96 well plates (1×10^4 cells / well) in 100 µl medium and let incubation for 24 hrs before the experiment. Serial dilutions of the chemicals protoporphyrin IX (PpIX) and protoporphyrin-dopamine conjugate (DPpIX) were prepared at a ratio of 1:1, 1:5, 1:15, 1:30. One plate was left in the dark for 20 min and the other one was irradiated for 20 min using a light source (10 Philips TLK 40W/10R lamps (λ_{max} 420 nm) having the light intensity 10mW/cm^2 measured by the photometer). Following exposure to the light, 24-hour cytotoxicities were determined with the (LDH) lactate dehydrogenase leakage assay (ROCHE), respectively. Cytotoxicity assay was performed according to the manufacture's instructions. Afterwards, absorbance was measured at 490 nm using the ELISA reader.

2.4 Cell Viability Assay

Hela, SH-SY5Y and U87 cell lines were seeded in duplicate 96 well plates (1×104 cells / well) in 100 µl medium and let incubation for 24 hrs before the experiment. Serial dilutions of the chemicals protoporphyrin IX (PpIX) and protoporphyrin-dopamine conjugate (DPpIX) were prepared at a ratio of 1:1, 1:5, 1:15, 1:30. One plate was left in the dark for 20 min and the other one was irradiated for 20 min using a lamp (10 Philips TLK 40W/10R lamps (λmax 420 nm) having the light intensity 10mW/cm^2 measured by the photometer). Following exposure to the light for 24 hrs cell proliferation assay was performed with the WST-1 reagent (ROCHE). Proliferation Assay was done according to the manufacture's instructions. Afterwards absorbance was measured at 450 nm using an ELISA reader.

2.5 Immunoflourescent Staining

2.5.1 Phosphatidylserine Localization

Hela and U87 cell lines were seeded in duplicate 96 well plates (7.5x10^3 cells / well) in 100 µl medium and let incubation for 24 hrs before the experiment. Serial dilutions of the chemicals protoporphyrin IX (PpIX) and protoporphyrin-dopamine conjugate (DPpIX) were prepared at a ratio of 1:5 and 1:15. One plate was left in the dark for 20 min and the other one was irradiated for 20 min using a lamp (10 Philips TLK 40W/10R lamps (λmax 420 nm) having the light intensity 10mW/cm2 measured by the photometer). Following exposure to the light for 24 hrs phosphatidylserine accumulation was determined with the Apoptosis Detection Kit, Annexin-V-Alexa 568 (ROCHE) according to the manufacture's instructions. The results were analyzed by fluorescent microscopy.

2.5.2 DNA Fragmentation

Hela and U87 cell lines were seeded in culture dishes (20x10^4 cells / well) in 5 ml medium and let incubation for 24 hrs before the experiment. Serial dilutions of protoporphyrin-dopamine conjugate (DPpIX) were prepared at a ratio of 1:5 and 1:15. One plate was left in dark for 20 min and the other one was irradiated for 20 min using a lamp (10 Philips TLK 40W/10R lamps (λ_{max} 420 nm) having the light intensity 10mW/cm^2

measured by the photometer). Following exposure to the light 24 hrs DNA fragmentation of cells were determined with the In Situ Cell Death Detection Kit, Fluorescein (ROCHE) according to the manufacture's instructions. The results were analyzed by confocal microscopy.

2.6 Reverse Transcription PCR

2.6.1 cDNA Synthesis

Caspase-3 was checked at the mRNA level. RT-PCR is a technique used to determine the change in mRNA concentration. Total RNAs of samples was extracted by using RNeasy kit (ROCHE). Then the total RNA concentrations of samples were quantified. 0.5 g of total RNA was reverse transcribed to obtain cDNA by Quantitect reverse transcription kit (Qiagen). cDNA underwent 30 or 35 cycles of amplification (PCR core kit, Qiagen). To prepare the genomic DNA elimination reaction, 14 µL reverse transcription master mix , 2 µL of gDNA Wipeout Buffer , and the volume of RNA corresponding to 0,5 g were added in eppendorf tube and then volume was completed to 14 µL with RNase-DNase free water. Then the tube was incubated for 2 min at 42 °C and by following this, tube was placed on ice. The reverse-transcription master mix was obtained by adding of 1 µL RT Primer Mix, 4 µL Quantiscript RT Buffer and Quantiscript Reverse Transcriptase on the mixture to obtain totally 20 µL volume ice. Then, the tube was incubated at 42°C for 15 min. To inactivate Quantiscript Reverse Transcriptase, tube was incubated for 3 min at 95°C.

2.6.2 RT-PCR

A 25 µL reaction was prepared by mixing 1 µL of cDNA, 16.8 µL of double distilled water, 0.2 µL of Taq polymerase, 0.5 µL of 10 mM dNTP, 2 µL of 25 mM MgCl2, 1 µL of forward primer, 1 µL of reverse primer and 2.5 µL of 10X Buffer. The PCR conditions were 5 min at 94 °C for initial incubation, 30 sec at 94 °C for denaturation, 45 sec at 58 °C for annealing of Caspase-3 primer, 1 min at 72 °C for extension and 7 min at 72 °C final incubation. The PCR was done for 35 cycles.

Content	Volume
10 X Buffer	2.5 µl
25 mM $MgCl_2$	2 µl
10 mM dNTP	0,5 µl
F.Primer	1µl
R.Primer	1µl
Taq Polimerase	0.2 µl
cDNA	1 µl
ddH_2O	16,8 µl

2.6.3 Gel Electrophoresis

Agarose gel electrophoresis is used to separate PCR products according to their sizes. To visualize the products under UV light safe DNA staining solution were used. To prepare 2 % (w/v) agarose gel, 1.6 g of agarose powder (Sigma) and 80 ml of 0.5 X TBE buffer (Fluka) were added an erlenmayer flask and boiled in microwave oven. Then the flask was cooled and 12µl/80ml safe DNA staining solution was added. Just before it solidifies comb is placed in order to generate 20 wells into 13 x 14x 0.5 horizontal agarose gel platform and then the solution was poured. 100 bp DNA Ladder (Bioron) was used as molecular size marker. To load PCR products on gel, bromophenol blue loading dye was used. Gel was run at 110 V for 45 min. The bands were visualized in Bio Rad gel doc.

CHAPTER 3

RESULTS

3.1 Cytotoxicity Assay

Irradiation induced cytotoxic effect of PpIX and DPpIX on HeLa, SH-SY5Y and U87 cell lines was measured with LDH cytotoxicity kit. Graphs observed in the figure represent three independent experiments performed in triplicate assays.

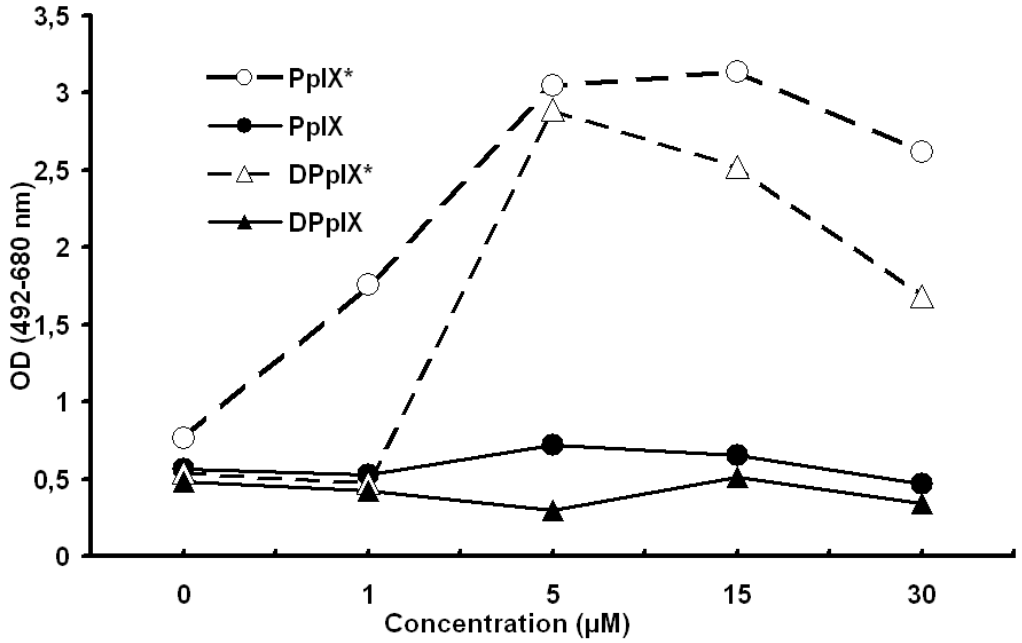

Figure 3.1 Irradiation induced cytotoxic effect of PpIX and DPpIX on HeLa cell line. Graphs observed in the figure represent three independent experiments performed in triplicate assays. The figure depicted the effect of 0-30 µg/ml PpIX and DPpIX treated for 24 hrs with and without irradiation (PpIX* and DPpIX*: irradiated; PpIX and DPpIX: unirradiated).

A)

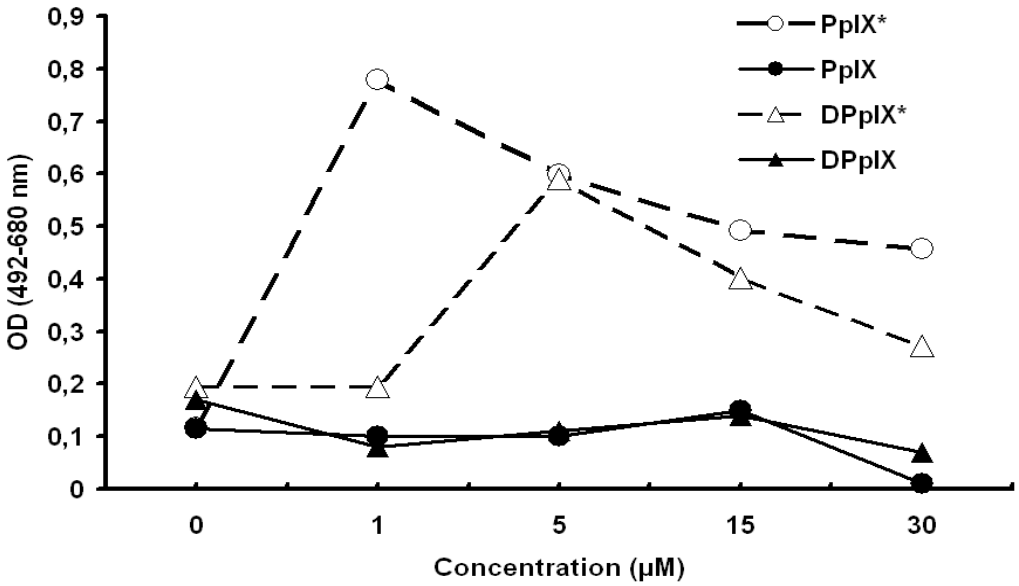

B)

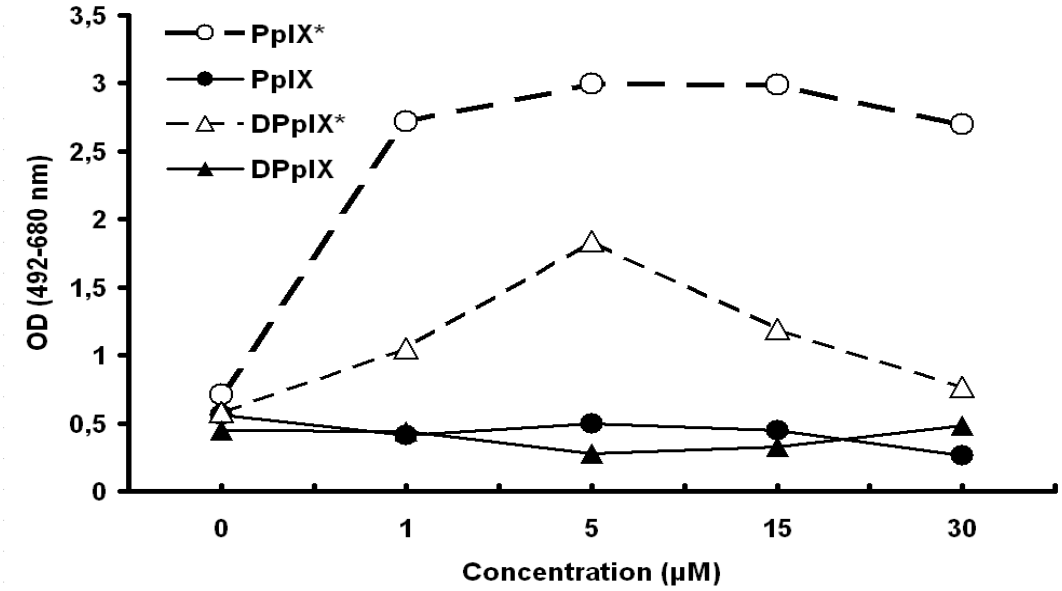

Figure 3.2 Irradiation induced cytotoxic effect of PpIX and DPpIX on SH-SY5Y and U87 cell lines. Graphs observed in the figure represent three independent experiments performed in triplicate. (A) SH-SY5Y and (B) U87 cell lines. The figures depicted the effect of 0-30 µg/ml PpIX and DPpIX treated for 24 hrs with and without irradiation (PpIX* and DPpIX*: irradiated; PpIX and DPpIX: unirradiated).

PpIX and DPpIX caused membrane damage and reduced the proliferation of cancer cells significantly**.** Three different human cancer cell lines, HeLa, Neuroblastoma SHSY5Y and U87, were used to examine the cytotoxic effects of PpIX

and DPpIX with and without irradiaiton. HeLa was chosen as a type of human carcinoma, neuroblastoma SHSY5 as dopaminergic cells [24, 25] and U87 as a glioblastoma. The integrity of the plasma membrane was evaluated by an LDH assay after 24 hrs incubation of cells with 0, 1, 5, 15 and 30 μM PpIX. At indicated hrs of post-irradiation time, irradiated cells rendered significantly higher LDH increase as compared to the negative control cells (untreated samples). PpIX*(irradiated) and DPpIX* (irradiated) demonstrated similar cytotoxic effects on the three different cell lines indicated in Figures 3.1 and 3.2. The ability of PpIX* and DPpIX* to induce cell death, release of LDH into the culture medium, increased in a dose-dependent manner up to 5 or 15 μM depending on the cell type and then become stabilized and decreased at higher, 30 μM, concentration. These cytotoxic effects revealed by a significant increase of LDH release in the culture medium were not associated with irradiation itself (irradiated cells in the absence of PpIX and DPpIX). Moreover, no effects of PpIX and DPpIX were found on the levels of LDH under unirradiated conditions. Indeed, similar levels of LDH were found in the culture medium of untreated cells and of unirradiated cells cultured in the presence of PpIX and DPpIX.

3.2 Proliferation Assay

The anti-proliferative effects of PpIX and DPpIX on HeLa, SH-SY5Y and U87 cell lines were measured with WST-1 proliferation assay kit. The results are shown in Figure 3.3 and Figure 3.4.

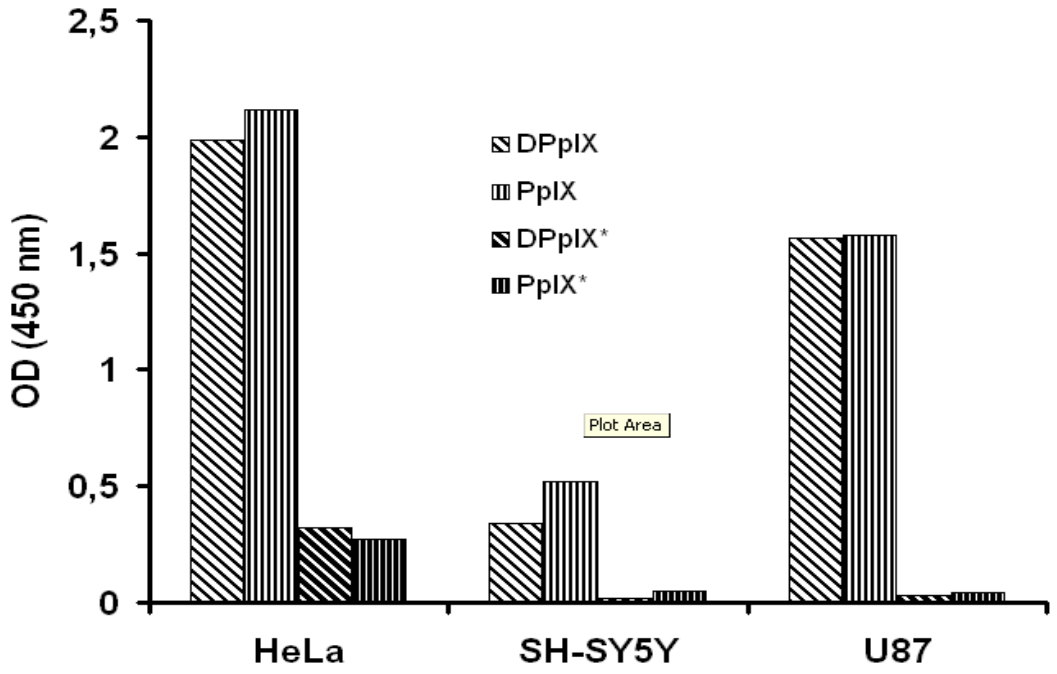

Figure 3.3 Results of the proliferation assay of 5 μg/ml of PpIX and DPpIX. PpIX and DPpIX treated for 24 hrs with and without irradiation (PpIX* and DPpIX*: irradiated).

The idea based on the analysis of the viable cells by cleavage of the tetrazolium salts into formazan by cellular enzymes is performed to elucidate the effect of the PpIX* and DPpIX* on the proliferation of the cancer cells. We established similar experimental set up as we did for LDH assay to compare the proliferation rates of the cells treated with 5μM of the PpIX* and DPpIX* after 24 hrs of treatment. Cell viability graph of the irradiated and unirradiated samples revealed that cell viability of treated cells decreased significantly compared to the PpIX and DPpIX treated cells. PpIX* and DPpIX* demonstrated similar inhibition effect on the proliferation of the cell lines indicated in Figure 3.3.

3.3 DNA Fragmentation

The detection of DNA fragmentation of DPpIX for PDT-treated and non-treated HeLa cells was assessed using the TUNEL assay at 20 min.

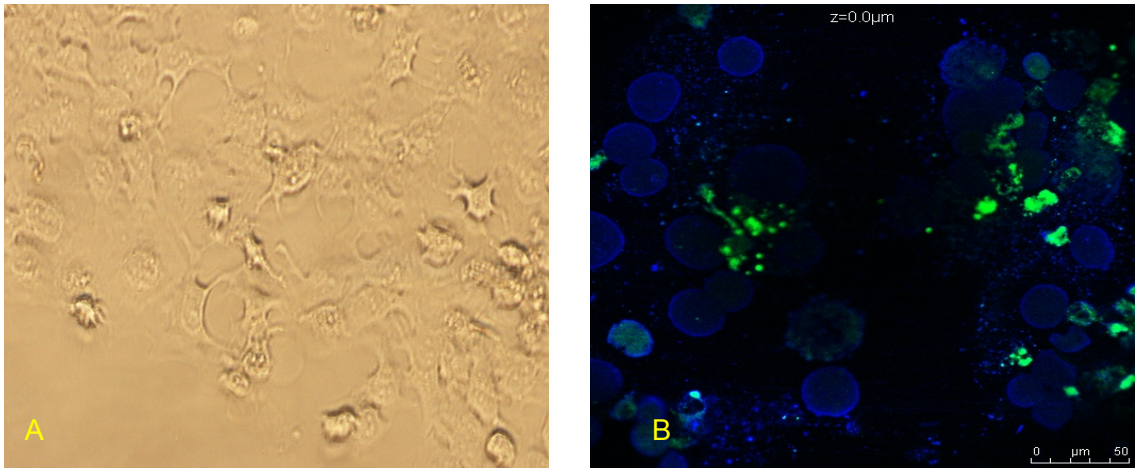

Figure 3.4 Positive control Camptotechin-treated HeLa cells observed under A) invert light and B) confocal microscopes. Images are at A) 20X and B) 40X.

Figure 3.4 A shows the shrinkage of Camptotechin treated HeLa cells under invert light microscope. DPpIX treated HeLa cells were assesed using the TUNEL assay as seen in Figure 3.4 B. Camptotechin was used as a positive control. A green fluorescent signal was observed. %50 ± of the Camptotechin treated HeLa cells underwent apoptosis.

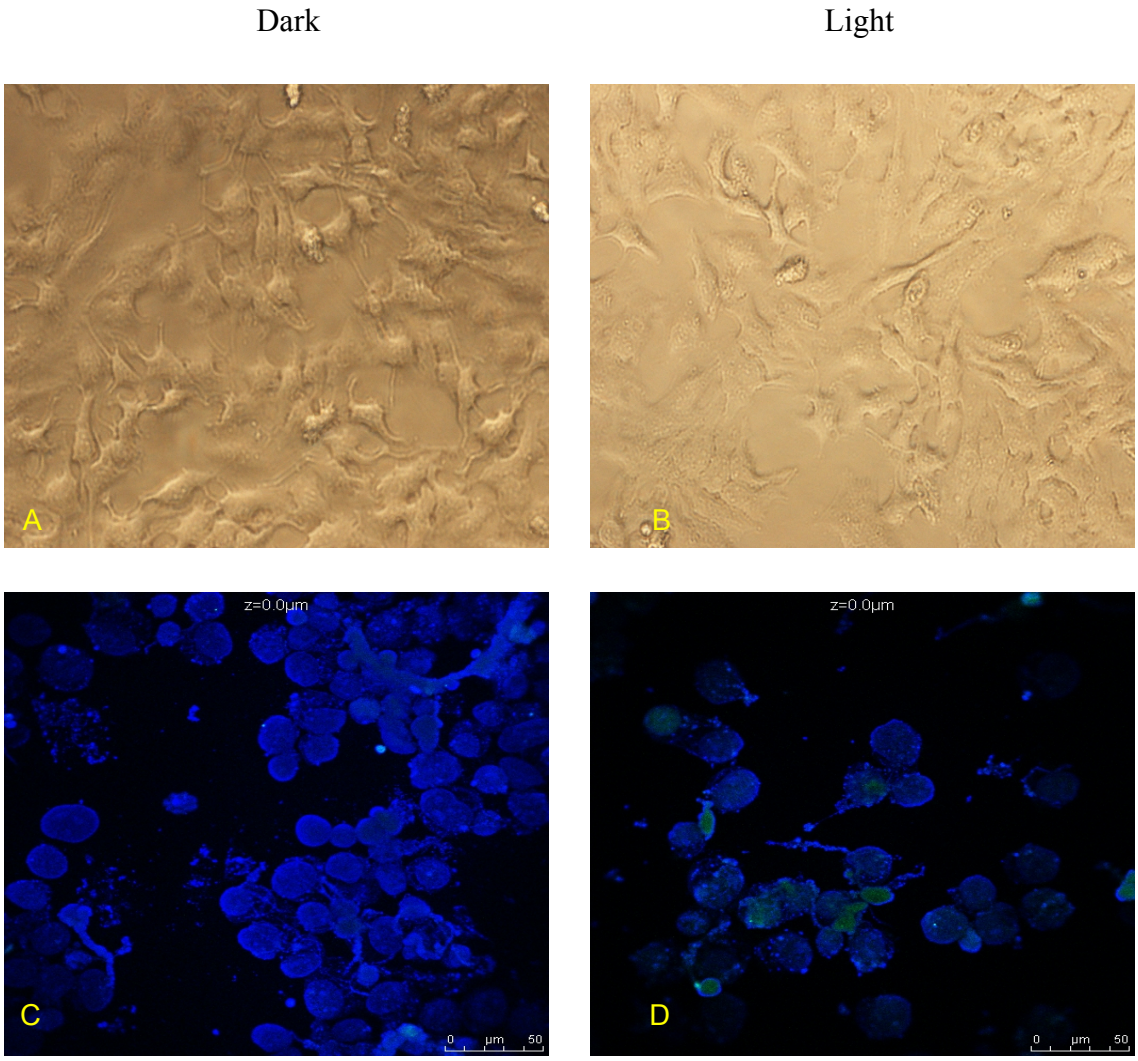

Figure 3.5 HeLa cells observed under light and confocal microscopes. The fluorescence images seen in c and d were obtained as a result of TUNEL assay. A) Control without PDT under invert light microscope, B) Control with PDT under invert light microscope, C) Control without PDT under confocal microscope, D) Control with PDT under confocal microscope. Images are at 20X (A and B) and 40X (C and D).

The morphology of the control cells did not change under any circumstances. The presence of light did not cause any significant effect (Figure 3.5a and b) as observed in light microscopy. TUNEL assay was applied to the control cells treated with and without light. There were no green fluorescence signals in the cells with no irradiation whereas the cells with irradiation showed only a small level of green fluorescence. Under light conditions %13 ± of the cells underwent apoptosis.

Dark Light

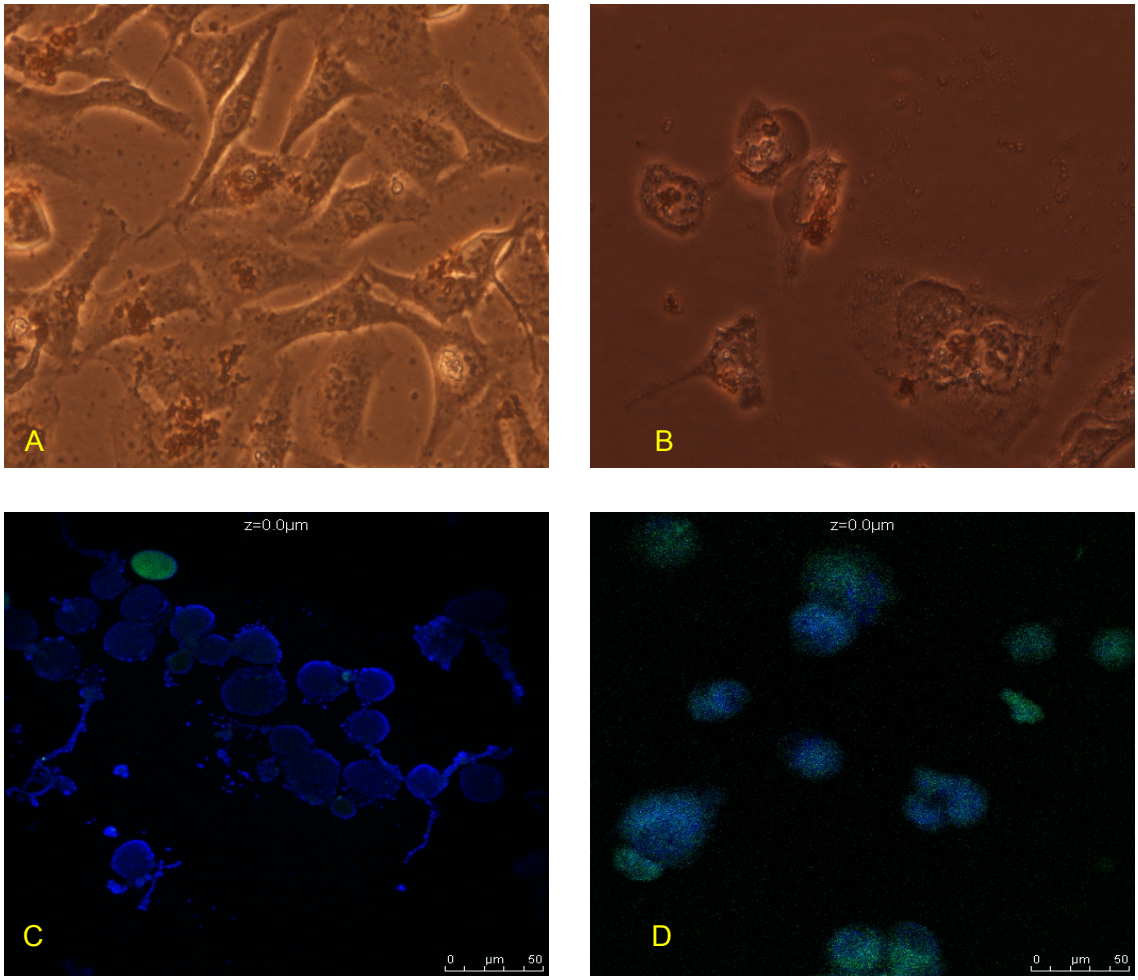

Figure 3.6 Apoptosis assay of HeLa cells which are treated 5 µM DPpIX observed under invert light microscope for A and B, and confocal microscope for C and D. A) Images are at 20X (A and B) and 40X (C and D).

The HeLa cells were treated with 5 µM DPpIX. There is no change in the morphology of the cells in dark while cell shrinkage and cytoplasmic degradation took place in light (Figure 3.6 a and b). The TUNEL assay was applied to 5 µM DPpIX treated HeLa cells with and without irradiation. Almost no green fluorescent signal was observed in dark and just %4 ± of the cells underwent apoptosis. In contrast, upon light treatment, HeLa cells were labeled with green fluorescence and %70 ± of the cells underwent apoptosis. These data revealed that, under PDT-treatment, almost all cells undergo apoptosis while just a few cells undergo apoptosis with no PDT-treatment.

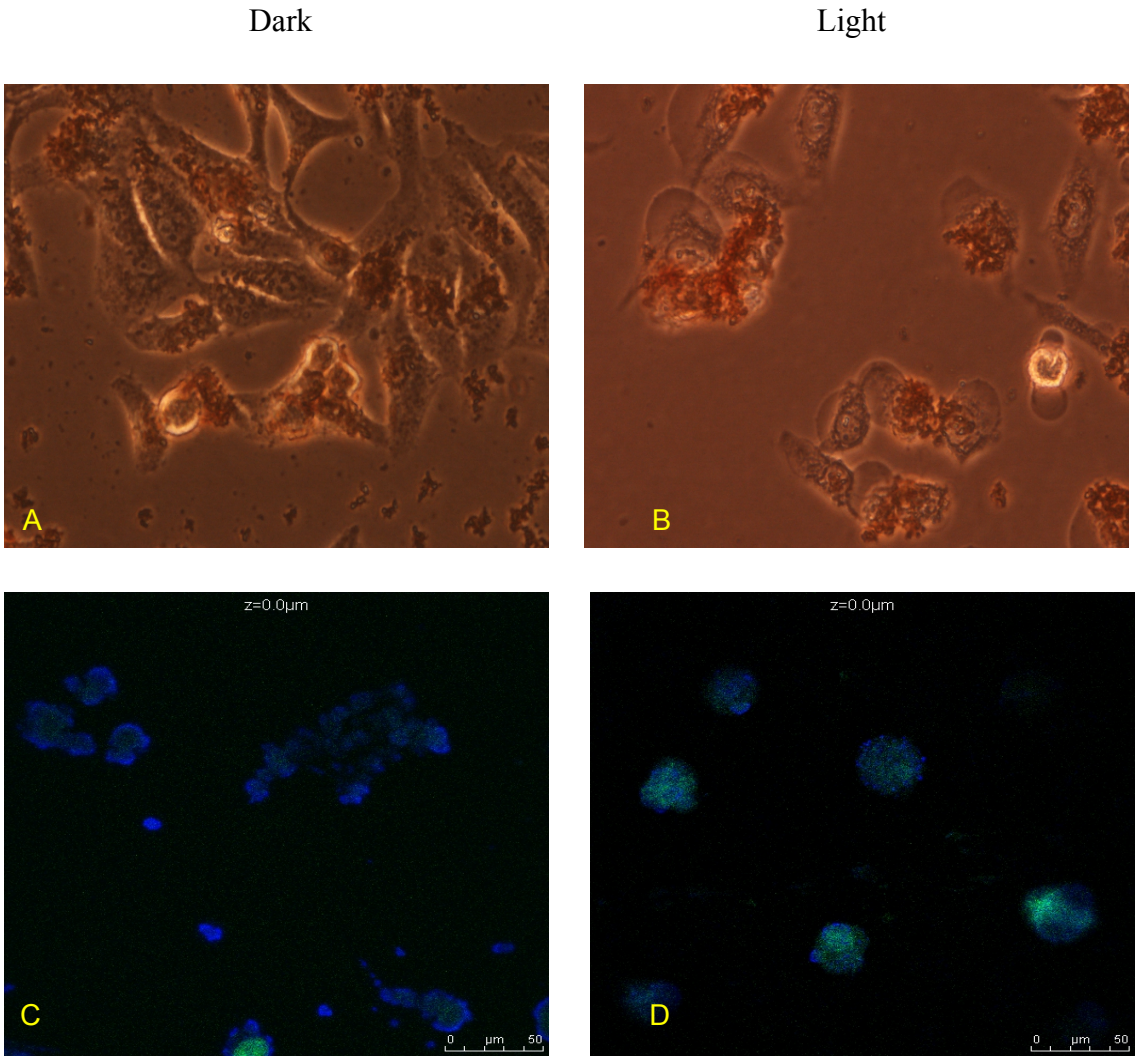

Figure 3.7 Apoptosis assay of HeLa cells which are treated 15 µM DPpIX observed under invert light microscope for A and B, and confocal microscope for C and D. A) Images are at 20X (A and B) and 40X (C and D).

When the HeLa cells were treated with 15 µM DPpIX, no changes in the morphology of the cells in dark were observed while cell shrinkage and cytoplasmic degradation took place in light (Figure 3.7 a and b). The TUNEL assay was applied to 15 µM DPpIX treated HeLa cells with and without irradiation. Almost no fluorescent signal was observed in dark and %60 ± of the cells underwent apoptosis. In contrast, upon light treatment, HeLa cells were labeled with green fluorescence and %96 ± of the cells underwent apoptosis.

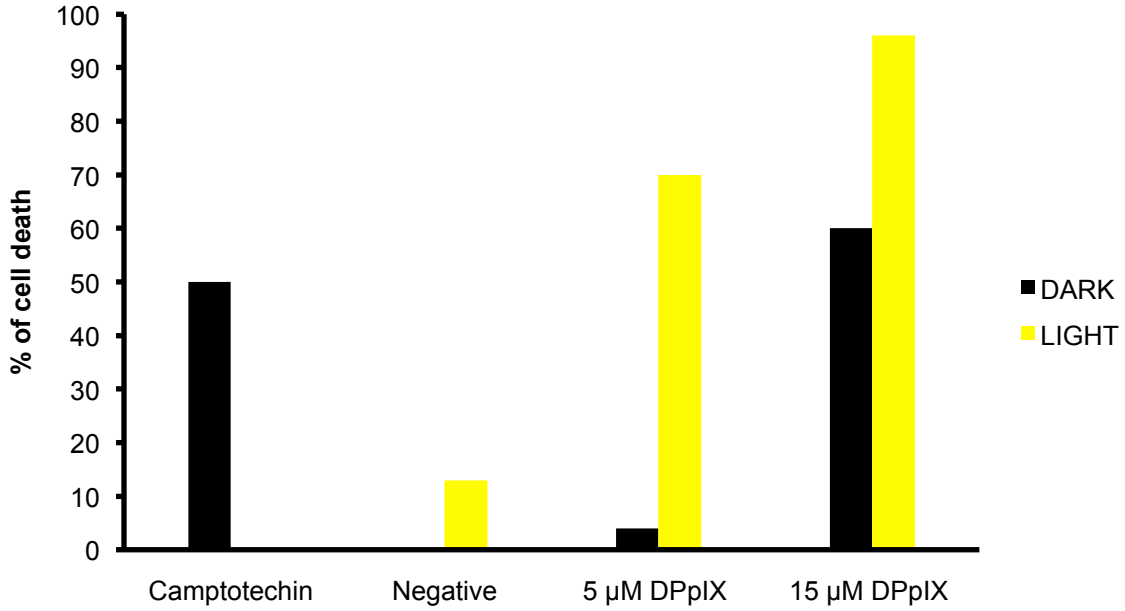

Figure 3.8 % of cell death observed in 5 and 15 µM DPpIX treated HeLa cells.

3.4 Phosphotidylserine Localization

The distruption of the cell membrane and the release of phosphotidylserine which are indications of apoptosis were observed with Annexin-V –Alexa 568 assay kit. The results were observed with fluorescence microscopy.

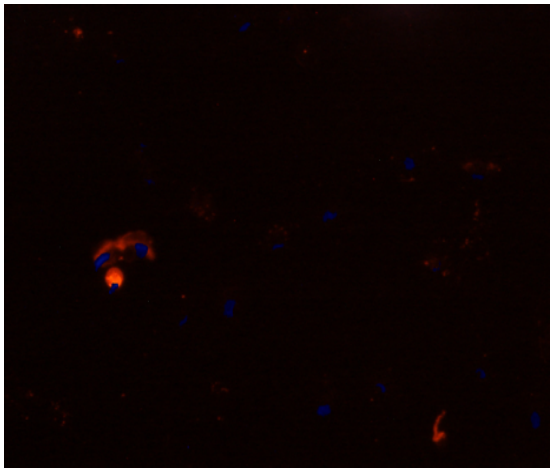

Figure 3.9 The fluorescence image of HeLa cells treated with Camptotechin for 30 s exposure.

Camptotechin was used as a positive control for apoptosis assay. Annexin-V Alexa 568 assay kit was applied to Camptotechin treated HeLa cells.

Dark Light

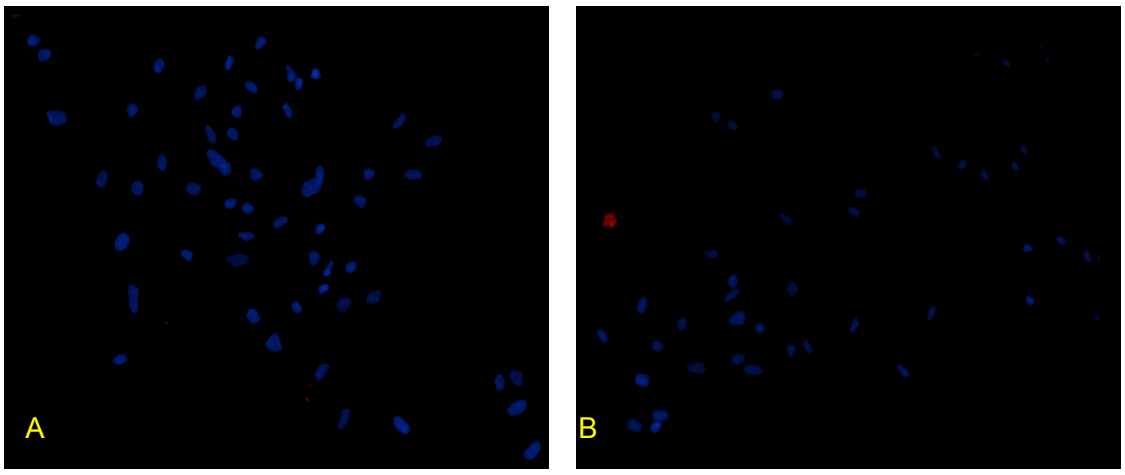

Figure 3.10 DAPI merge. Results of Annexin-V assay of HeLa cells under fluorescence microscopy A) without irradiation, and B) with irradiation. Exposure time=30 s.

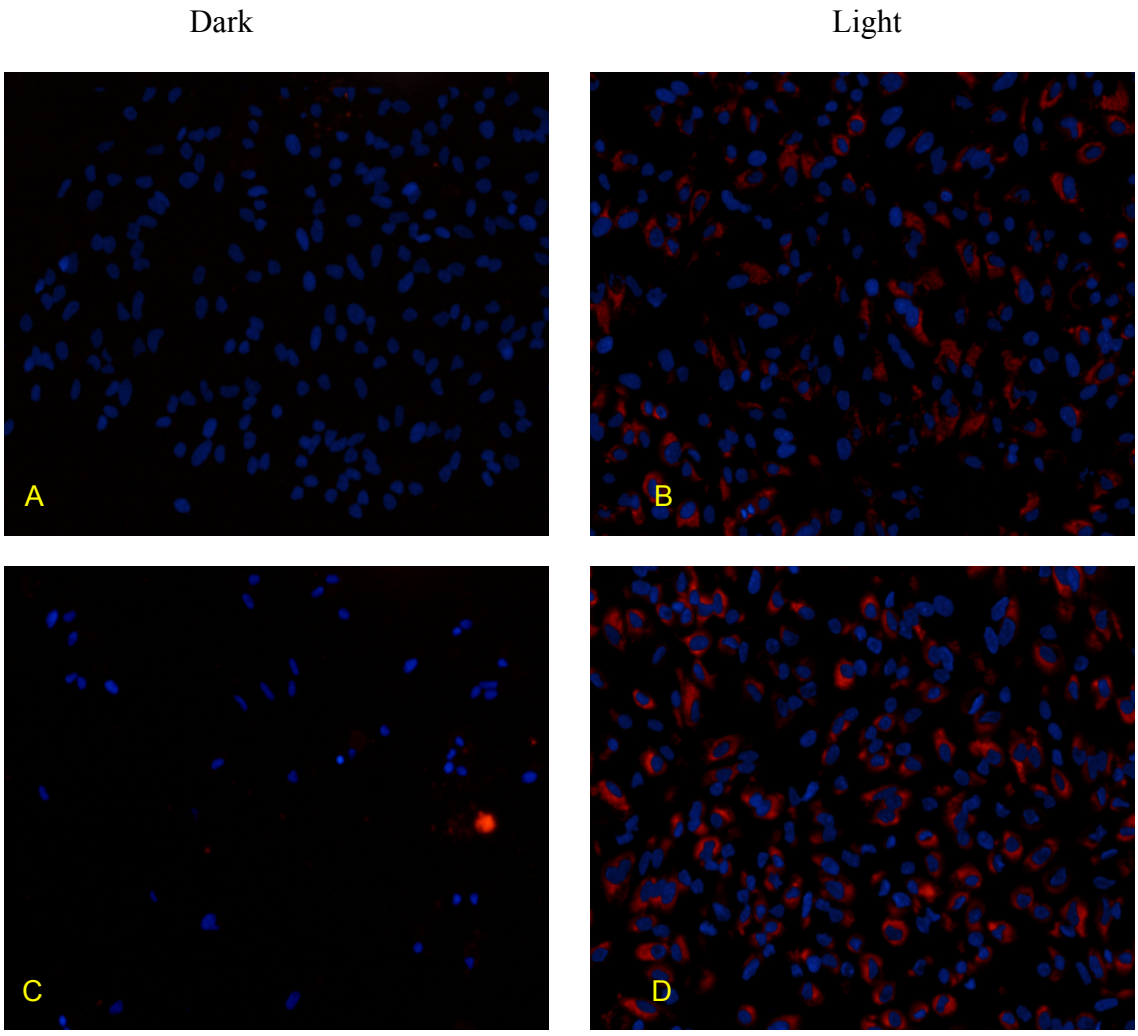

Figure 3.11 Results of Annexin-V assay of HeLa cells. A-B) 30 s exposure fluorescence microscope images of HeLa cells treated with 5 µM PP-IX in dark and light. C-D) 30 s exposure fluorescence microscope images of HeLa cells treated with 5 µM DPpIX in dark and light.

The Annexin assay was applied to 5 µM PP-IX treated HeLa cells with and without irradiation. Almost no red fluorescent signal was observed in dark and %5 ± of the cells underwent apoptosis. In contrast, upon light treatment, HeLa cells were labeled with red fluorescence and %70 ± of the cells underwent apoptosis.

In 5 µM DPpIX treated HeLa cells almost no red fluorescent signal was observed in dark and %10 ± of the cells underwent apoptosis. In contrast, upon light treatment, HeLa cells were labeled with red fluorescence and %94 ± of the cells underwent apoptosis.

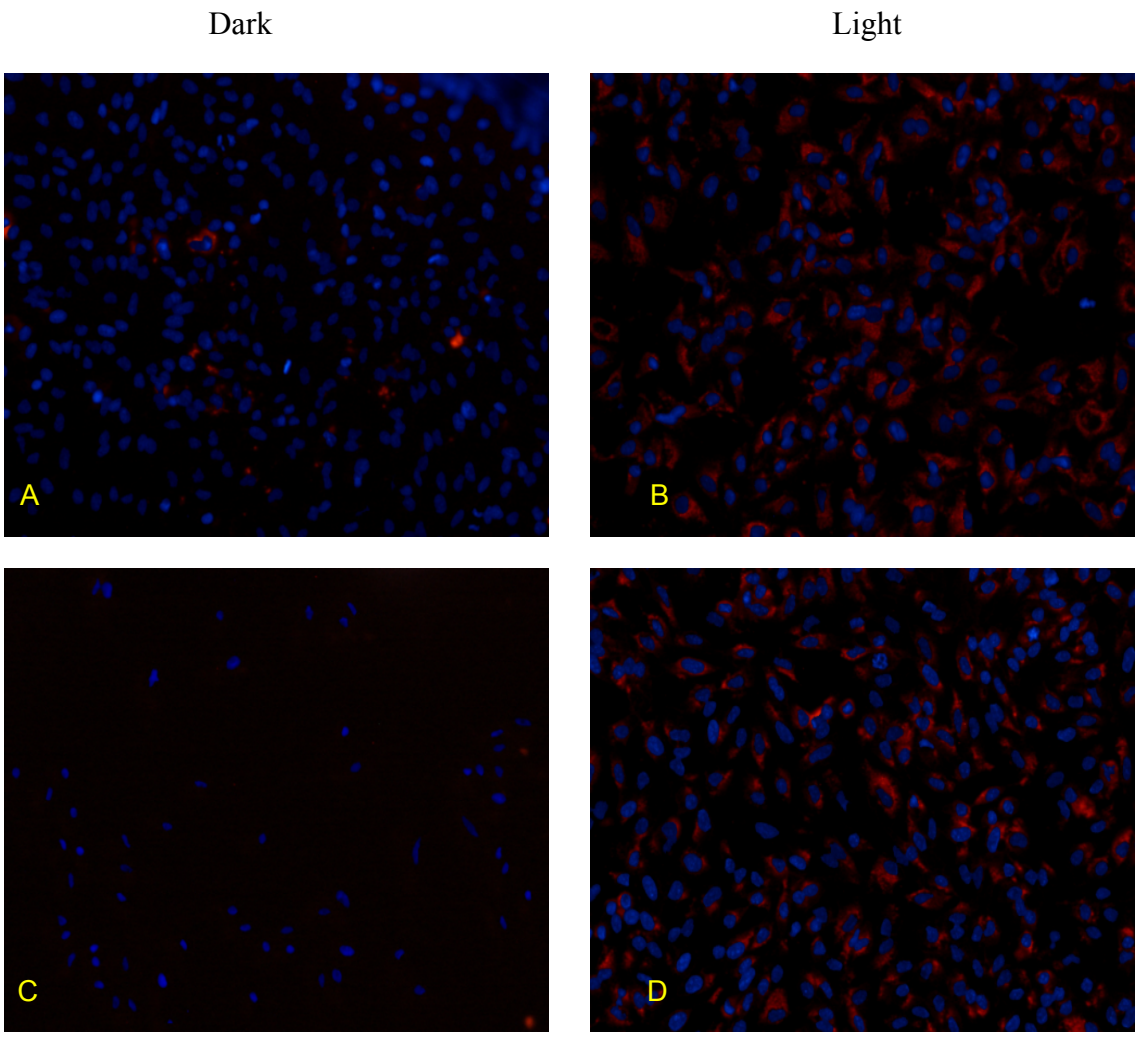

Figure 3.12 Results of Annexin-V assay of HeLa cells. A-B) 30 s exposure fluorescence microscope images of HeLa cells treated with 15 µM PP-IX in dark and light. C-D) 30 s exposure fluorescence microscope images of HeLa cells treated with 15 µM DPpIX in dark and light.

The Annexin assay was applied to 15 µM PP-IX treated HeLa cells with and without irradiation. Almost no red fluorescent signal was observed in dark and %4 ± of the cells underwent apoptosis. In contrast, upon light treatment, HeLa cells were labeled with red fluorescence and %98 ± of the cells underwent apoptosis.

In 15 µM DPpIX treated HeLa cells almost no red fluorescent signal was observed in dark and %1 ± of the cells underwent apoptosis. In contrast, upon light treatment, HeLa cells were labeled with red fluorescence and %96 ± of the cells underwent apoptosis.

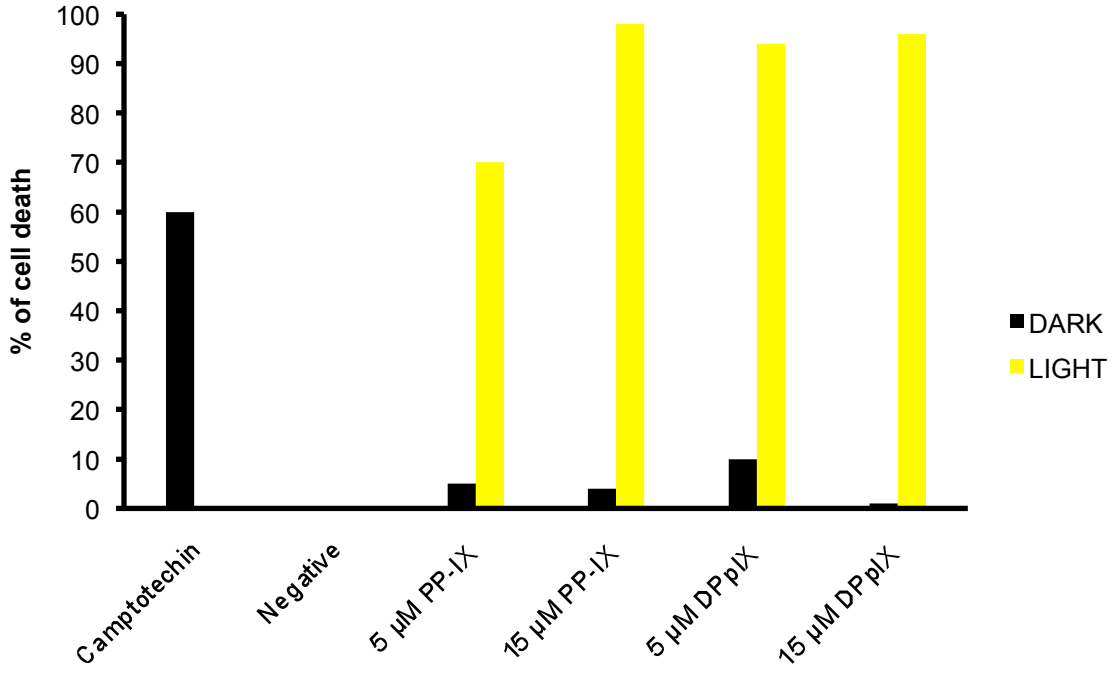

Figure 3.13 % of cell death in HeLa cells treated with 15 µM PP-IX in dark and light.

30 s

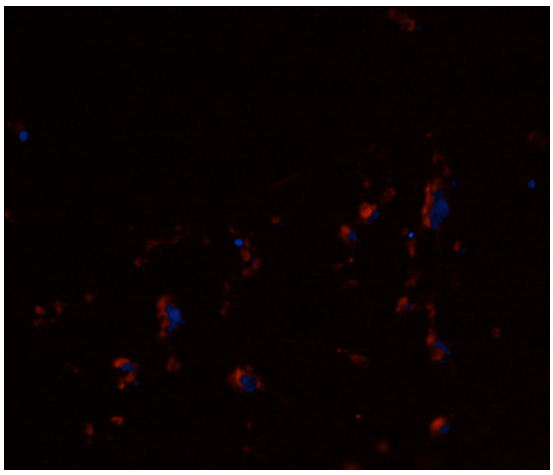

Figure 3.14 The fluorescence images of U-87 cells treated with Camptotechin for 30 s exposure time.

Dark

Light

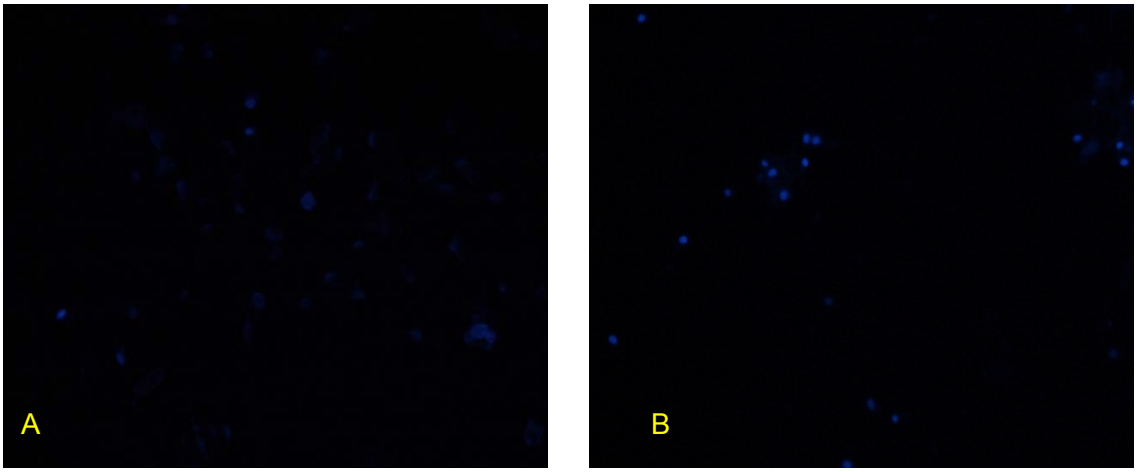

Figure 3.15 Results of Annexin-V Alexa assay of U87 cells. Fluorescence microscope images of control U87 cells. Exposure time = 30 s.

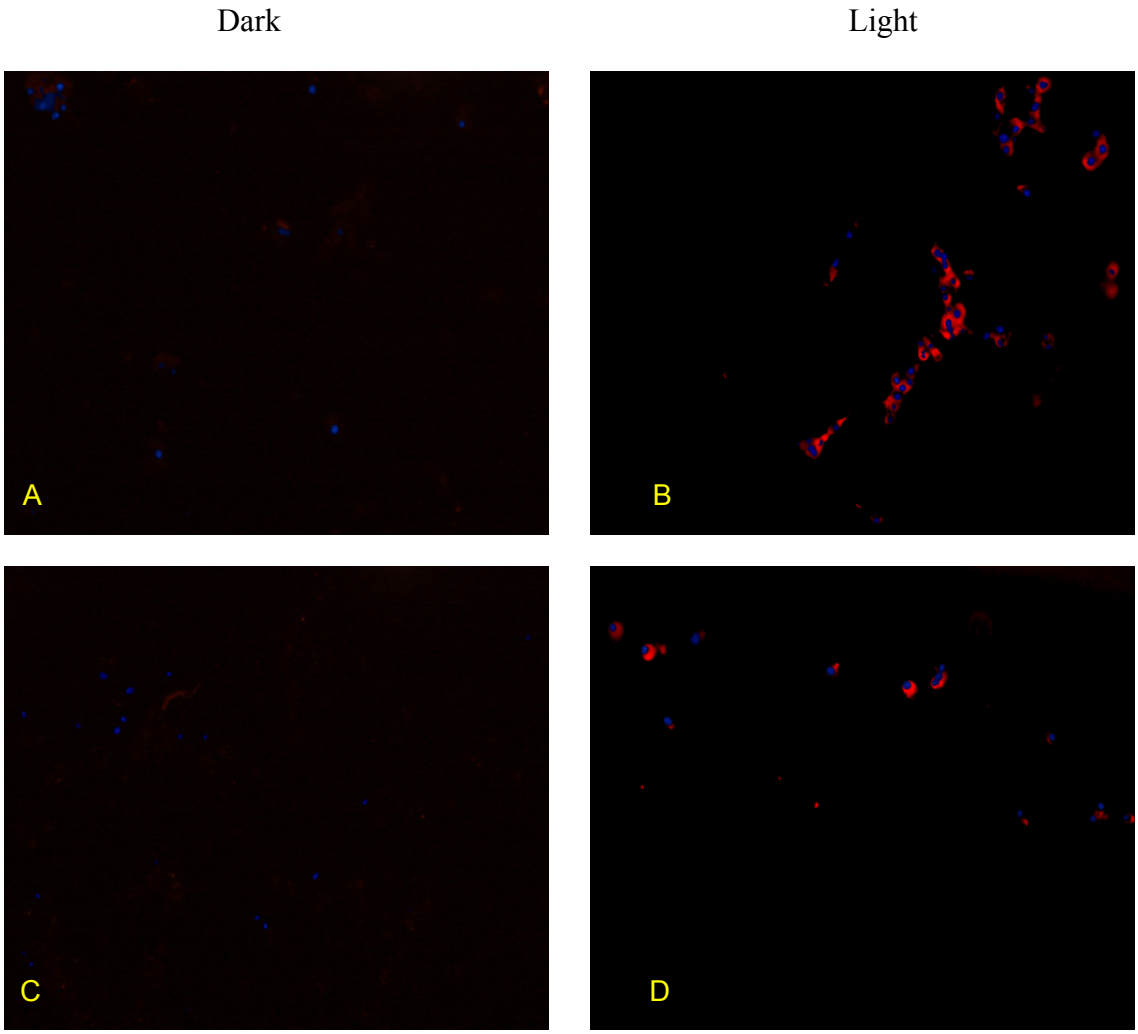

Figure 3.16 Results of Annexin-V assay of U-87 cells. A-B) 30 s exposure fluorescence microscope images of U-87 cells treated with 5 µM PP-IX in dark and light. C-D) 30 s exposure fluorescence microscope images of U-87 cells treated with 5 µM DPpIX in dark and light.

The Annexin assay was applied to 5 µM PP-IX treated U-87 cells with and without irradiation. Almost no red fluorescent signal was observed in dark and %40 ± of the cells underwent apoptosis. In contrast, upon light treatment, U-87 cells were labeled with red fluorescence and %96 ± of the cells underwent apoptosis.

In 5 µM DPpIX treated U-87 cells almost no red fluorescent signal was observed in dark and %10 ± of the cells underwent apoptosis. In contrast, upon light treatment,

U-87 cells were labeled with red fluorescence and %96 ± of the cells underwent apoptosis.

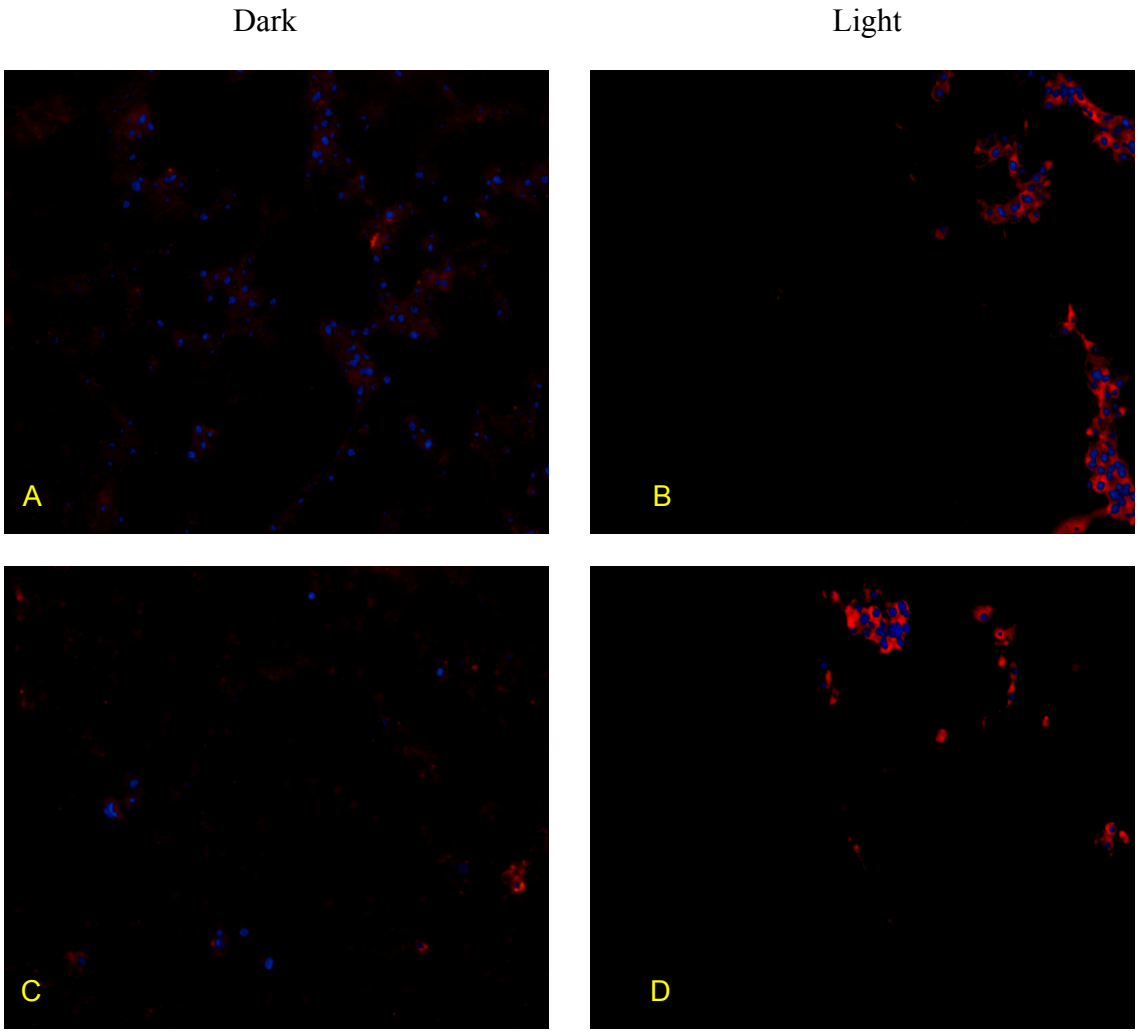

Figure 3.17 Results of Annexin-V assay of U-87 cells. A-B) 30 s exposure fluorescence microscope images of U-87 cells treated with 15 µM PP-IX in dark and light. C-D) 30 s exposure fluorescence microscope images of U-87 cells treated with 15 µM DPpIX in dark and light.

The Annexin assay was applied to 15 µM PP-IX treated U-87 cells with and without irradiation. Red fluorescent signal was observed in dark and %97 ± of the cells underwent apoptosis. Upon light treatment, U-87 cells were labeled with red fluorescence and %99 ± of the cells underwent apoptosis.

In 15 µM DPpIX treated U-87 cells almost no red fluorescent signal was observed in dark and %40 ± of the cells underwent apoptosis. In contrast, upon light

treatment, U-87 cells were labeled with red fluorescence and %98 ± of the cells underwent apoptosis.

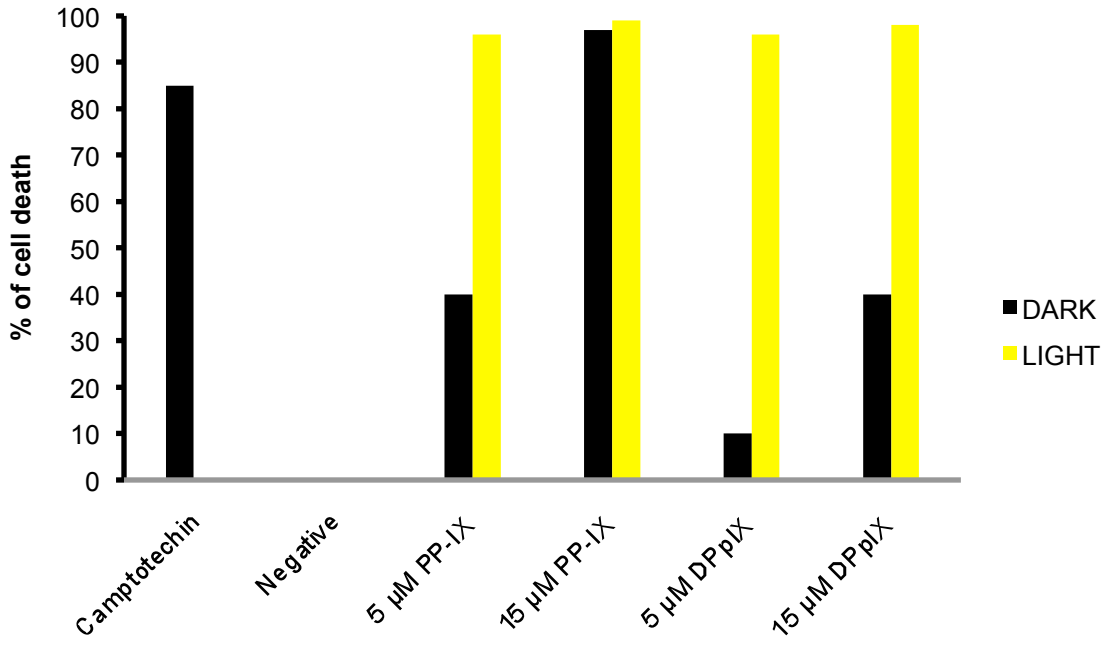

Figure 3.18 % of cell death in HeLa cells treated with 15 µM PP-IX in dark and light.

3.5 Caspase Activity

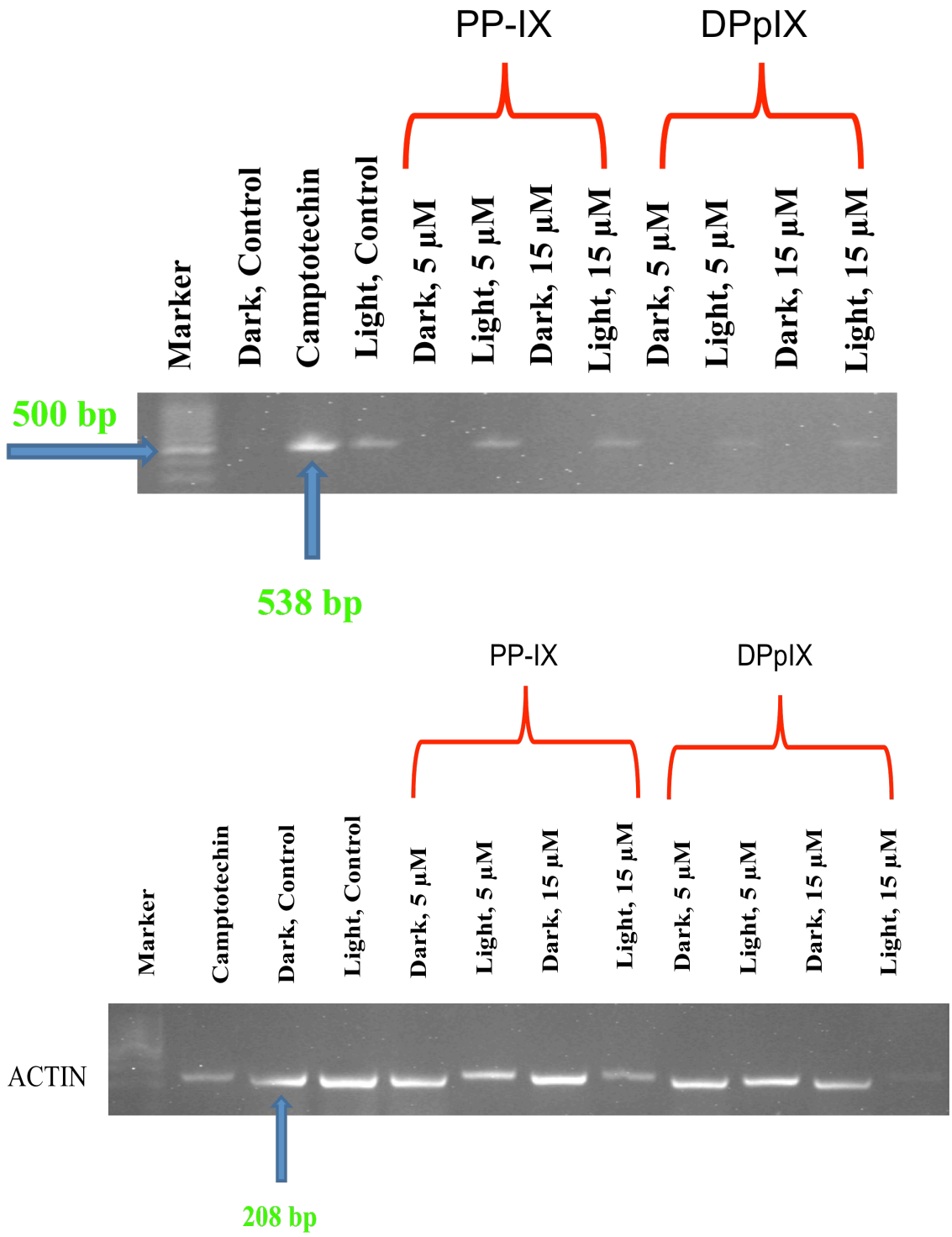

Figure 3.19 Caspase-3 and Actin expressions of U-87 cells.

We assayed the caspase-3 activity in the cells treated with 5 μM and 15 μM concentrations of Protoporphyrin-IX, dopamine-conjugate Protoporphyrin-IX individually along with control cells both with and without irradiation by RT-PCR. Actin was used as the positive control to test if cDNA worked properly. Under light conditions, Caspase-3 was expressed and a band formed. However, in dark, no bands were formed and thus Caspase-3 was not expressed.

CHAPTER 4

DISCUSSION

Although conventional cancer treatments such us radiation therapy, surgery, and chemotherapy are effective, they do not remove or destroy malignant cells which can metastasize later. The ongoing radiation and chemical therapies have serious side effects due to the loss of normal cell function because of comparatively indiscriminate cytotoxic properties. Another side effect of these treatments is that they are highly troublesome to the patient. Therefore new treatment methods that can discriminate normal and diseased tissue need to be developed. Biological therapies for cancer, angiogenesis inhibitor treatment, peripheral blood stem cell transplant, bone marrow transplant and gene therapy for cancer, laser treatment, PDT and targeted cancer therapies are some of the new treatments. Among those, PDT is a promising technique to fight cancer. Photodynamic therapy, PDT, is a promising modality to combat cancer. Although it has almost been 30 years since it was first proposed as a functional therapeutic approach in oncology, PDT has only found more widely use in clinical practice [58]. A lot of advances in the understanding of the biology and chemistry of this treatment technique have taken place and improved photosensitizers are under development. Modern systems for light delivery are available, too [29].

There are several advantages of PDT over surgery and radiotherapy: it is less invasive, it has reduced side effects, it is applicable even in areas previously exposed to ionizing radiation, healing times are relatively shorter, has comparable clinical outcome, the treatment of various lesions simultaneously is possible, repeating the procedure with no tumor resistance development risk and positive cost-effectiveness outcome. When assessed in pre-clinical models, a lot of photosensitizers are kept in tumors to a greater degree than normal tissues [49].

Light, oxygen and a photosensitizer are the three fundamental requirements of PDT. The photosensitizer is chosen depending on the cancer type and injected into the bloodstream. Then the tumor is irradiated with appropriated light depending on the photosensitizer and the need to guarantee the maximum concentration in the malignant tissues. The photosensitizer absorbs the light and produces an active form of oxygen that destroys nearby cancer cells. The higher the oxygen concentration the better, but the success of the therapy is mostly related to the photosensitizer.

There are several *in vitro* studies of photosensitizers in the literature. Protoporphyrin-IX is one of them. It is known that Protoporphyrin IX decreases the rate of cell viability and induces apoptosis in HeLa cells prior to photodynamic treatment [8]. The other study at releated to photosensitizers is interaction of Protoporphyrin IX with wild-type p53 protein *in vitro* and induction of cell death in human colon cancer cells [57].

In this work, dopamine-conjugate Protoporphyrin-IX was synthesized to increase the specifity of the Protoporphyrin-IX and was examined if it shows dopaminergic effect on SH-SY5Y cell line or not. The effects of dopamine-conjugate Protoporphyrin-IX and protoporphyrin IX on the proliferation, cytotoxicity and apoptosis of SH-SY5Y, HeLa and U-87 cells were evaluated.

For the cytotoxicity assay, 1, 5, 15, and 30 μM concentrations of Protoporphyrin-IX and dopamine-conjugate Protoporphyrin-IX were tested on HeLa, SH-SY5Y and U-87 cells with and without irradiation. Irradiated cells released significantly higher LDH increase as compared to the negative control cells (untreated samples). We observed that Protoporphyrin-IX (irradiated) and dopamine-conjugate Protoporphyrin-IX (irradiated) have similar cytotoxic effects on these cells. Based on the results, 5 μM and 15 μM were chosen as the optimum doses of the chemicals. We confirmed that the cell viability decreases when the cells were treated with 5 μM concentration of Protoporphyrin-IX (irradiated) or dopamine-conjugate Protoporphyrin-IX (irradiated). Since SH-SY5Y cells are dopaminergic cells [55-56] dopamine-conjugate Protoporphyrin-IX was expected to have higher cytotoxic effect on SH-SY5Y cells. But our results were not as we expected. Both chemicals had higher cytotoxic and lower cell viability values in U-87 and HeLa cells. So we didn't use SH-SY5Y cells in our later assays.

It is known that some photosensitizers induce apoptosis *via* different mechanisms.

Cell membrane blebbing and phosphotidylserine localization are some of the indications of apoptosis that can be detected by specific markers, such as Annexin-V. Natalia et al. observed apoptosis in PP-IX treated cells with Annexin-V assay. We demonstrated that HeLa and U-87 cells go into apoptosis process by the detection of Annexin-V when these cells are treated with 5 μM and 15 μM concentrations of Protoporphyrin-IX or dopamine-conjugate Protoporphyrin-IX with and without irradiation. Camptotechin was used as a positive control as it definitely causes apoptosis. Untreated HeLa and U-87 cells both in dark and light were the negative controls in this study. The apoptosis levels in the non-irradiated cells treated with 5 μM and 15 μM concentrations of Protoporphyrin-IX or dopamine-conjugate Protoporphyrin-IX were very low compared with their irradiated counterparts. It is revealed that both Protoporphyrin-IX and dopamine-conjugate Protoporphyrin-IX cause apoptosis while there is not much difference in the apoptosis levels in the cells treated with the mentioned concentrations of them. Although there are some apoptotic cells treated with 5 μM and 15 μM concentrations of Protoporphyrin-IX or dopamine-conjugate Protoporphyrin-IX present in dark, this number is much higher in the ones in light.

There were no apoptotic features found in the negative control cells even with irradiation. This shows that PDT itself does not cause cells go into apoptosis.
DNA fragmentation is another evidence of apoptosis which is generally used in PDT investigations. Liu et al. detected DNA fragmentation following PDT-treatment using TUNEL assay [22].

According to the TUNEL assay results in our study, it is clearly revealed that the cells treated with 5 μM and 15 μM concentrations of Protoporphyrin-IX or dopamine-conjugate Protoporphyrin-IX displayed some morphological changes such as cell blebbing following their treatment with light. In contrast, no morphological changes in dark were observed. We obtained very similar results in TUNEL assay to the Annexin-V assay results which proves the apoptotic effect of Protoporphyrin-IX and dopamine-conjugate Protoporphyrin-IX at 5 μM and 15 μM concentrations on irradiated cancer cells.

The signaling pathways of caspase cascades are correlated with morphological and biochemical changes during apoptosis. We assayed the caspase-3 activity in the cells treated with 5 μM and 15 μM concentrations of Protoporphyrin-IX, dopamine-conjugate Protoporphyrin-IX individually along with control cells both with and without irradiation by RT-PCR. Actin was used as the positive control to test if cDNA worked properly. Under light conditions, Caspase-3 expression increased and had higher band densities. However, under unirradiated conditions, no bands were formed and thus Caspase-3 expression was not observed.

We confirmed apoptosis with three different methods which are annexin staining, tunel staining and caspase-3 activity.

CHAPTER 5

CONCLUSIONS

In our work, we have demonstrated that Protoporphyrin-IX and its dopamine conjugate Protoporphyrin IX induces apoptosis in different cancer cell lines by confirming apoptosis with three different methods: Annexin-V assay, TUNEL assay, and Caspase-3 activity detection. Based on our results, it can be concluded that Protoporphyrin-IX or dopamine-conjugate Protoporphyrin-IX at concentrations 5 μM and 15 μM can be used as photosensitizers and are effective PDT candidates in the treatment of cancer.

REFERENCES

[1] Figge, F. H., *et al.*, "Cancer detection and therapy; affinity of neoplastic, embryonic, and traumatized tissues for porphyrins and metalloporphyrins," *Proc Soc Exp Biol Med,* vol. 68, p. 640, Jul-Aug 1948.

[2] Lipson, R. L. and E. J. Baldes, "The photodynamic properties of a particular hematoporphyrin derivative," *Arch Dermatol,* vol. 82, pp. 508-16, Oct 1960.

[3] Kessel, D. and T. H. Chou, "Tumor-localizing components of the porphyrin preparation hematoporphyrin derivative," *Cancer Res,* vol. 43, pp. 1994-9, May 1983.

[4] Dougherty, T. J. *et al.*, "The structure of the active component of hematoporphyrin derivative," *Prog Clin Biol Res,* vol. 170, pp. 301-14, 1984.

[5] Dougherty, T. J. *et al.*, "Photoradiation therapy for the treatment of malignant tumors," *Cancer Res,* vol. 38, pp. 2628-35, Aug 1978.

[6] Dougherty, T. J. "Photosensitization of malignant tumors," *Semin Surg Oncol,* vol. 2, pp. 24-37, 1986.

[7] Dougherty, T. J. *et al.*, "Photodynamic therapy," *J Natl Cancer Inst,* vol. 90, pp. 889-905, Jun 17 1998.

[8] Bednarz, N. *et al.*, "Protoporphyrin IX induces apoptosis in HeLa cells prior to photodynamic treatment," *Pharmacol Rep,* vol. 59, pp. 474-9, Jul-Aug 2007.

[9] Gollnick, S. O. and C. M. Brackett, "Enhancement of anti-tumor immunity by photodynamic therapy," *Immunol Res,* vol. 46, pp. 216-26, Mar 2010.

[10] Simon, H. U., *et al.*, "Role of reactive oxygen species (ROS) in apoptosis induction," *Apoptosis,* vol. 5, pp. 415-8, Nov 2000.

[11] Sharman, W. M., *et al.*, "Role of activated oxygen species in photodynamic therapy," *Methods Enzymol,* vol. 319, pp. 376-400, 2000.

[12] Zhu, T. C. and J. C. Finlay, "The role of photodynamic therapy (PDT) physics," *Med Phys,* vol. 35, pp. 3127-36, Jul 2008.

[13] Szacilowski, K., *et al.*, "Bioinorganic Photochemistry: Frontiers and Mechanisms," *ChemInform,* vol. 36, pp. no-no, 2005.

[14] Ion, R., "Spectral studies of TSPP and TSNP used in PDT.I.Monomer-dimer equilibrium," *Rom. J. Biophys,* vol. 6, pp. 213–218 1996.

[15] Nowis, D.*, et al.*, "Direct tumor damage mechanisms of photodynamic therapy," *Acta Biochim Pol,* vol. 52, pp. 339-52, 2005.

[16] L. Lite Pharm Tech Co. (2010, *Mechanisms of PDT Tumor Destruction*.

[17] Rastogi, R. a. R. P. S. Rajesh P., "Apoptosıs: molecular mechanısms and pathogenıcıty," *EXCLI Journal,* vol. 8, pp. 155-181, 2009.

[18] Oleinick, N. L.*, et al.*, "The role of apoptosis in response to photodynamic therapy: what, where, why, and how," *Photochem Photobiol Sci,* vol. 1, pp. 1-21, Jan 2002.

[19] P. Dash. (2000, Apoptosis. Available: www.sgul.ac.uk/dept/immunology/~dash)

[20] Almeida, R. D., *et al.*, "Intracellular signaling mechanisms in photodynamic therapy," *Biochimica et Biophysica Acta (BBA) - Reviews on Cancer,* vol. 1704, pp. 59-86, 2004.

[21] Huang, H. F., *et al.*, "Mitochondria-dependent apoptosis induced by a novel amphipathic photochemotherapeutic agent ZnPcS2P2 in HL60 cells," *Acta Pharmacol Sin,* vol. 26, pp. 1138-44, Sep 2005.

[22] Liu, T., *et al.*, "Targeted photodynamic therapy for prostate cancer: inducing apoptosis via activation of the caspase-8/-3 cascade pathway," *Int J Oncol,* vol. 36, pp. 777-84, Apr 2010.

[23] van Heerde, W. L., *et al.*, "Markers of apoptosis in cardiovascular tissues: focus on Annexin V," *Cardiovasc Res,* vol. 45, pp. 549-59, Feb 2000.

[24] Akematsu, T. and H. Endoh, "Role of apoptosis-inducing factor (AIF) in programmed nuclear death during conjugation in Tetrahymena thermophila," *BMC Cell Biology,* vol. 11, p. 13, 2010.

[25] Fadok, V. A., *et al.*, "Exposure of phosphatidylserine on the surface of apoptotic lymphocytes triggers specific recognition and removal by macrophages," *J Immunol,* vol. 148, pp. 2207-16, Apr 1 1992.

[26] Andree, H. A.*, et al.*, "Binding of vascular anticoagulant alpha (VAC alpha) to planar phospholipid bilayers," *J Biol Chem,* vol. 265, pp. 4923-8, Mar 25 1990.

[27] Martin, S. J., *et al.*, "Early redistribution of plasma membrane phosphatidylserine is a general feature of apoptosis regardless of the initiating stimulus: inhibition by overexpression of Bcl-2 and Abl," *J Exp Med,* vol. 182, pp. 1545-56, Nov 1 1995.

[28] Star, W. M., *et al.*, "Destructive effect of photoradiation on the microcirculation of a rat mammary tumor growing in "sandwich" observation chambers," *Prog Clin Biol Res,* vol. 170, pp. 637-45, 1984.

[29] Huang, Z., *et al.*, "Photodynamic therapy for treatment of solid tumors--potential and technical challenges," *Technol Cancer Res Treat,* vol. 7, pp. 309-20, Aug 2008.

[30] Krammer, B., "Vascular effects of photodynamic therapy," *Anticancer Res,* vol. 21, pp. 4271-7, Nov-Dec 2001.

[31] Savellano, M. D., *et al.*, "Multiepitope HER2 targeting enhances photoimmunotherapy of HER2-overexpressing cancer cells with pyropheophorbide-a immunoconjugates," *Cancer Res,* vol. 65, pp. 6371-9, Jul 15 2005.

[32] Staneloudi, "Development and characterization of novel photosensitizer: scFv conjugates for use in photodynamic therapy of cancer.," *Immunology,* vol. 120, pp. 512-517, 2007.

[33] Qiang, Y.-G., *et al.*, "Combination of photodynamic therapy and immunomodulation: Current status and future trends," *Medicinal Research Reviews,* vol. 28, pp. 632-644, 2008.

[34] Castano, A. P., *et al.*, "Photodynamic therapy and anti-tumour immunity," *Nat Rev Cancer,* vol. 6, pp. 535-545, 2006.

[35] Brown, S. B., *et al.*, "The present and future role of photodynamic therapy in cancer treatment," *Lancet Oncol,* vol. 5, pp. 497-508, Aug 2004.

[36] Arménio, "A look at clinical applications and developments of photodynamic therapy," *Oncol Rev,* vol. 2, pp. 235-249, 2008.

[37] Nayak, "Photodynamic therapy in dermatology.," *Indian J. Dermatol. Venereol. Leprol. ,* vol. 71, pp. 155-160, 2005.

[38] Schuitmaker, "Photodynamic therapy: A promising new modality for the treatment of cancer.," *J. Photochem. Photobiol.,* vol. 34, pp. 3-12, 1996.

[39] Juzeniene, "Milestones in the development of photodynamic therapy and fluorescence diagnosis.," *Photochem. Photobiol. Sci.,* vol. 6, pp. 1234-1245, 2007.

[40] Ying, "Structure, Spectroscopy, and Reactivity Properties of Porphyrin Pincers: A Conceptual Density Functional Theory and Time-Dependent Density Functional Theory Study," *J. Phys. Chem.,* vol. 112, pp. 305-311, 2008.

[41] Macdonald, "Basic principles of photodynamic therapy," *Journal of Porphyrins and Phthalocyanines.*, vol. 5, pp. 105-129, 2001.

[42] Murakami, "Molecular recognition in anisotropic media. Binding of alkylpyridines to amphiphilic zinc porphyrins incorporated in liposomal bilayer membranes" *Org. Biomol. Chem., ,* vol. 7, pp. 1437-1444, 2009.

[43] Dougherty, "Photodynamic therapy," *J. Natl. Cancer Inst.,* vol. 90, pp. 547–561, 1998.

[44] Susmita, "Protoporphyrin IX-induced structural and functional changes in human red blood cells, haemoglobin and myoglobin " *Journal of Biosciences,* vol. 29, pp. 281-291, 2004.

[45] Pazos, M. C., and H. B. Nader, "Effect of photodynamic therapy on the extracellular matrix and associated components," *Braz J Med Biol Res,* vol. 40, pp. 1025-35, Aug 2007.

[46] Jianming, "Syntheses of protoporphyrin-IX derivatives bearing extended propionate side-chains," *NIH Public Access,* vol. 5, pp. 5-16, 2010.

[47] Chatterjee, "Nanoparticles in photodynamic therapy: an emerging paradigm.," *Adv Drug Deliv Rev. ,* vol. 60, pp. 1627-37, 2008.

[48] Kemikli, "Synthesis of protoporphyrin coated superparamagnetic iron oxide nanoparticles via dopamine anchor " *Journal of Alloys and Compounds,* vol. 502, pp. 439-444, 2010.

[49] Jia, Z. and X. Wan, "Concentration of protoporphyrin IX in cancer tissues and blood in patients with colorectal cancer at early stage," *Zhong Nan Da Xue Xue Bao Yi Xue Ban,* vol. 34, pp. 846-9, 2009.

[50] Kwitniewski, M.*, et al.*, "Influence of diamino acid derivatives of protoporphyrin IX on mouse immunological system: preliminary results," *J Photochem Photobiol B,* vol. 81, pp. 129-35, Dec 1 2005.

[51] Sol*,* V. *et al.*, "Amino porphyrins as photoinhibitors of Gram-positive and -negative bacteria," *Bioorg Med Chem Lett,* vol. 14, pp. 4207-11, Aug 16 2004.

[52] Gupta, A. K. and M. Gupta, "Synthesis and surface engineering of iron oxide nanoparticles for biomedical applications," *Biomaterials,* vol. 26, pp. 3995-4021, Jun 2005.

[53] Tayyaba Hasan, Anne C E Moor, and Bernard Ortel, "Photodynamic Therapy of Cancer," in *Holland-Frei Cancer Medicine*. D. W. B. R. C. H. W. N. H. W. K. P. R. E. W. R. R. H. J. F. F. E. Kufe, Ed. Ontario: B.C. Becker, 2000.

[54] Kristian Berg, ‘’Photosensitizers in medicine’’, Department of radiation biology. http://www.photobiology.info/Berg.html

[55] Oh-hashi, K., *et al.*, "Mitogen-Activated Protein Kinase Pathway Mediates Peroxynitrite-Induced Apoptosis in Human Dopaminergic Neuroblastoma SH-SY5Y Cells," *Biochemical and Biophysical Research Communications,* vol. 263, pp. 504-509, 1999.

[56] Deng, H., *et al.*, "Small interfering RNA targeting the PINK1 induces apoptosis in dopaminergic cells SH-SY5Y," *Biochemical and Biophysical Research Communications,* vol. 337, pp. 1133-1138, 2005.

[57] Zawacka-Pankau, J., *et al.*, "Protoporphyrin IX interacts with wild-type p53 protein in vitro and induces cell death of human colon cancer cells in a p53-dependent and -independent manner," *J Biol Chem,* vol. 282, pp. 2466-72, Jan 26 2007.

[58] Brown, S. B., *et al.*, "The present and future role of photodynamic therapy in cancer treatment," *Lancet Oncol,* vol. 5, pp. 497-508, Aug 2004.

[59] STEBA Biotech N.V. http://www.prostatepdt.com/pdt1.aspx

[60] Ortel, B., *et al.*, "Molecular mechanisms of photodynamic therapy," *Front Biosci,* vol. 14, pp. 4157-72, 2009.

[61] http://www.biocompare.com/Articles/ApplicationNote/866/In-Situ-Cell-Death-Detection-Kit.html